

Final Report Addendum

Characterization of Contaminant Migration Potential Through In-Place Sediment Caps

SERDP Project ER-1370

June 2011

Philip Gidley
Seokjoon Kwon
Upal Ghosh
University of Maryland Baltimore County

This document has been cleared for public release



I. TABLE OF CONTENTS

I. Executive Summary	2
II. Research Objectives	3
III. Background	4
IV. Materials and Methods	9
i. Sediment and capping material source	9
ii. Solid-Phase Micro Extraction (SPME) for PAH measurements	9
iii. Batch equilibrium measurements.	10
iv. PAH Analysis by Gas Chromatography-Mass Spectrometry	10
v. Column studies	11
vi. Modeling contaminant transport	13
vii. Numerical solution for the NAPL dissolution model	15
V. Results and Accomplishments	18
i. Characterization of sediment and capping materials	18
ii. Sediment-water equilibrium measurement.	20
iii. Column studies without amendments	22
iv. Column studies with amended caps	25
v. Aqueous equilibrium experiments with sediment before and after flushing with water.	31
vi. PAH Migration in Biological Column Experiments	33
vii. Modeling PAH migration in sediment caps	38
VI. Conclusions and future recommendations	47
VII. List of publications	49
VIII. References	51

I. Executive summary

By isolating contaminated sediments, capping can effectively reduce exposure to contaminants and the potential for contaminant transport into the food chain. However, typical sand caps have little sorption capacity to retard the transport of hydrophobic contaminants such as PAHs that can be mobilized by groundwater flow. The primary objective of this research was to develop and improve engineering tools for more efficient cap designs by enhancing the scientific understanding of organic contaminant transport through sediment caps and the role of sorbent amendments in enhancing cap performance. Laboratory column experiments were performed using contaminated sediments and capping materials obtained from a creosote contaminated EPA Superfund site. The study examined activated carbon and peat moss amendments to the cap as ways to enhance contaminant retardation.

Laboratory column experiments demonstrated rapid breakthrough of lower molecular weight PAHs in experimental columns when groundwater upflow is simulated through a cap. Within a few bed volumes of flow, all 12 PAHs measured were found to break through the 60 cm of capping material. PAH concentration in the capping material was low and comparable to background levels typically seen in depositional sediment, but the porewater concentrations were high. A key conclusion of this comparison is that measurement of PAH concentration in cores taken out of sediment caps is a poor indicator of contaminant breakthrough, especially in cases where there is little capacity in the cap material to trap contaminants. In-situ porewater concentrations need to be measured to provide an assessment of contaminant movement through caps. Column experiments with a natural organic matter (peat moss) delayed PAH breakthrough in the cap. The most dramatic result was observed for caps amended with activated carbon at a dose of 0.2 and 2% by weight. PAH concentrations in the cap pore water in the activated carbon amended caps were several orders of magnitude lower than concentrations in the porewater in the source sediments even after several hundred bed volumes of flow. Thus, enhancing the sorption capacity of caps with activated carbon amendment even at a low dose appears to make a major impact on the quality of porewater achieved in the cap. Sediment caps with and without biological activity did not show remarkable difference for the flow conditions tested. However, mathematical simulation of much slower flowrates expected in the field indicated a bigger impact of biodegradation on PAH migration. It is also possible that in the long-term over many years, a biological community in the form of biofilms may develop in the capping material that adds to the effectiveness of the cap. However, this could not be observed in the short-term (several months) of laboratory experiments.

It is critical to note that scientifically appropriate performance criteria needs to be chosen to monitor the performance of a capping remedy. For example, if PAH concentration in the cap is the criteria, an unamended sand cap that allows PAH laden groundwater to flow through and contaminate the overlying surface water may look superior to a carbon amended cap that adsorbs the migrating PAHs and retains the contaminants in the cap keeping the surface water protected. Long-term mathematical simulations demonstrated that even at a very small dose of GAC amendment (0.002%) to a sand cap, breakthrough is delayed to 10 years and with 0.2% AC, the breakthrough is longer than 1000 years. It is possible that mass transfer limitations within carbon particles and fouling of the carbon with other organic molecules may degrade long-term performance to some extent. However, with the large reductions in PAH transport evident from the laboratory experiments and modeling simulations with GAC amended sand caps, it appears promising to include GAC amendments in sand caps to enhance performance where groundwater advection is of concern.

II. Research Objectives

The primary objective of this research was to develop and improve engineering tools for more efficient cap designs by enhancing the scientific understanding of organic contaminant transport through sediment caps. To achieve this objective, the following research questions were addressed:

1. Can pore water movement due to groundwater potential enhance contaminant mobilization and influence long-term effectiveness of sediment caps for the protection of benthic and aquatic environments?
2. Can improved understanding of actual porewater concentrations and contaminant binding in natural or engineered capping materials enhance predictive capability of cap performance and facilitate more effective cap design?
3. Can selection of an appropriate natural capping material and amending the sorptive capacity with sorbents (e.g., activated carbon), ensure long-term contaminant stability and minimize vertical contaminant transport where advective processes are of concern?

These research questions were addressed by performing laboratory measurements of PAH transport processes and mathematical modeling. Laboratory column experiments were performed using contaminated sediments and capping materials obtained from a creosote contaminated EPA Superfund site. The study examined activated carbon and peat moss amendments to the cap as ways to enhance contaminant retardation. The study used innovative laboratory tools, analytical techniques, and numerical modeling to build on the current knowledge of contaminant transport through caps. PAHs are the model contaminants in this study, but findings here for PAHs could be transferred to other hydrophobic organic contaminants.

III. Background

By isolating contaminated sediments, capping can effectively reduce exposure to contaminants and the potential for contaminant transport into the food chain. One third of the 60 Tier I contaminated sediment sites in the United States involve capping and about 20% of the tier 1 sites involve PAHs (<http://www.epa.gov/superfund/health/conmedia/sediment/data.htm>). The sources of PAH contamination in sediments are typically from coal and petroleum processing and use. Many contaminated freshwater and marine sediment sites reside in shallow, near shore areas that are often impacted by advective processes (e.g., groundwater flow, tidal pumping, and wave pumping), benthic bioturbation, and hydrodynamic forces. These forces contribute to the flux of contaminants through sediments. Current cap design methods do not adequately account for contaminant transport processes and for organic content and type when selecting capping materials and designing cap thicknesses, despite the known significant impact of organic matter on contaminant sorption and transport. Material selection criteria are based primarily on cap stability considerations (Palermo, Clausner et al. 1998), affected largely by surface water hydrodynamic forces, and most caps are conservatively designed based on a theoretical understanding of contaminant transport.

Current state of art in sediment cap design is documented in the US EPA capping guidance (Palermo, Maynard et al. 1998) and the US Army Corps of Engineers Capping Guidance Document (Palermo, Clausner et al. 1998). Cap design guidance in these documents focuses on establishing sufficient cap thickness to protect benthic organisms by isolating contaminated sediments beneath a sufficiently thick layer of clean sand. Although the potential for contaminant transport through sediment caps is acknowledged in these design documents, it is not included as a design criterion. The following key features were identified from the guidance documents and from a review of historically placed caps:

- Caps normally are composed of clean sediment (these are commonly referred to as sand caps)
- Contaminant transport in a cap may be predicted using a model that describes contaminant transport through a porous medium
- 1-D models often assume sorption equilibrium, using sorption coefficients calculated from contaminant partition coefficient (K_d , measured or estimated from K_{ow})
- Possible use of activated carbon as sand cap amendment is mentioned, but the documents do not include discussions of experimental studies or how such amendments should be designed and placed.

A submerged cap provides physical isolation of the contaminated sediment by preventing re-suspension and distances benthic communities from the pollution source. This remediation method is suited for areas with minimal currents, waves, ship traffic and ice, to allow for long term cap integrity (Palermo, M.R., Clausner. et al., 1998). It has been shown that capping is effective when diffusive forces are the primary mechanism by which contaminants are transported in the porewater (Murphy, P., et al., 2006; Thoma, G.J., et al., 1993; Eek, E., et al. 2008) Advection during tidal pumping (Simpson, S.L. et al. 2002) and groundwater discharge (Viana, P.Z. et al. 2008; Burnett, W.C., et al., 2003; Liu, C., et al., 2001; Boehm, A.B. et al. 2004) can adversely affect cap performance. A literature review by Liu et al. (2001) showed that specific discharge rates of submarine flow range from 1.08×10^{-6} to 0.3 m/hr. It is likely that the high discharge rates are during low tide and are not averaged over high and low tide periods. In general, average specific discharge rates greater than 1×10^{-4} m/hr are considered high. At Hood Canal, WA average groundwater discharge rates were measured to be 0.036 m/hr (Swarzenski, P.W, 2007). Groundwater advection could lead to the transport of metals (Viana, P.Z. et al. 2008) and organics such as polycyclic aromatic hydrocarbons (PAHs) (Hyun, S. et al. 2006) and polychlorinated biphenyls (PCBs) (Murphy, P. et al. 2006).

Hydrodynamic, sorptive, and geotechnical conditions within the cap need to be designed to minimize contaminant flux to the surface water (Mohan R.K., et al., 2000; Wright, S.J., et al. 2001). Some capping approaches have tried to minimize contaminant flux by diverting the upwelling groundwater away from the contaminated sediment (Barth E. F., et al., 2008). A sediment cap that is impermeable will do little to minimize long term risk at sites of potential groundwater discharge if contaminated groundwater flows around the cap. At the Wyckoff, Eagle Harbor Superfund site in Washington, groundwater seepage has been observed (averaged 0.001 m/hr in one of two locations measured), and the migration of polycyclic aromatic hydrocarbons (PAHs) may be greatly increased by advective processes in some areas (Magar, V.S. et al. 2007). The site was a wood processing facility and is the source of creosote contamination (<http://yosemite.epa.gov/R10/CLEANUP.NSF/sites/Wyckoff>). PAHs in the creosote are known to cause a variety of adverse biological effects in marine fish. After capping the site with sediment and sand, indicators of flatfish health (e.g. biliary fluorescent aromatic compounds, hepatic DNA adducts, and lesion risk) have been improving for 11 years (Myers, M.S. et al. 2008).

Biological activity in sediment caps. It has been demonstrated that bacteria can colonize capping material in column experiments (Himmelheber, D.W. et al. 2009). In situations where tidal pumping is

occurring, it is conceivable that oxygen might be carried from the surface to serve as a terminal electron acceptor (TEA). Oxygen and nutrients have the greatest influence on the effectiveness of PAH degradation in sand caps (Hyun, S. et al. 2006). With PAHs of molecular weight greater than pyrene, degradation may be limited even in aerated conditions (Hyun, S. et al. 2006). Within both sediment and cap layers of the columns, bioavailability, and consequently degradation of PAHs will be proportional to the number of aromatic rings and alkyl substitutions (White, H.K., et al. 2005).

In marine environments, sulfate would also be supplied from the surface sea water and serve as a TEA. Research has suggested that sulfate reduction is the most relevant for anaerobic marine sediments (Coats, J.D. et al. 1996; Rothermich, M.M. 2002). In the case of groundwater discharge or upwelling, it would be expected that oxygen concentrations would be limited to levels found in typical groundwater (~0.5 mg/L). Groundwater could supply nitrate for nitrate reduction (Swarzenski, P.W., et al. 2007; McNally, N.L. et al. 1998). The porewater from the capping material at Eagle Harbor measured high nitrate levels (66 mg/L) after being stored for 3 years at 4 degrees C. Groundwater typically has much lower nitrate levels (~1mg/L). Other terminal electron acceptors have been detected in caps, with bacterial community composition correlated to depth, Fe^{2+} , and Mn^{2+} concentration gradients in the cap (Himmelheber, D. W., et al. 2009).

Microbially mediated redox conditions could increase the amount of humic acid liberated as dissolved organic matter (DOM) (Kim, H.S. et al. 2005) and could therefore influence PAH transport through columns. Experiments have been performed using peat moss amendments to degrade gasoline and BTEX (benzene, toluene, ethyl-benzene and m-, o-, p-xylenes) compounds under microaerophilic conditions (Yerushalmi, L. et al. 1999). While the most rapid degradation occurs while oxygen is present, studies have shown the anaerobic degradation of some low molecular weight PAHs such as naphthalene and 2-methylnaphthalene can be significant if porewater levels of sulfate are maintained at 14-25mM (Rothermich, M.M., et al. 2002). Porewater concentrations of the Eagle Harbor capping material was measured to be 13mM as shipped (again after being stored in a fridge at 4 degrees C for 3 years). This concentration will decrease if freshwater discharge is occurring.

Role of sorbents in sediment caps. Sand caps are permeable, but have little ability to sequester organics (Murphy, P., et al. 2006), and do not provide conditions to form insoluble metal sulfides (Simpson, S.L., et al. 2002). A variety of capping amendments are being explored to increase sequestration of metals and organics in sand caps. Apatite and organoclay have the broadest range of effectiveness for metals (Viana, P.Z. et al. 2008), while activated carbon, coke (Zimmerman et al. 2004;

Murphy, P., et al. 2006), peat (Rasmussen, G. et al. 2002), and organoclays (Viana, P.Z., et al. 2008) are being explored for organics. Major factors controlling sorption of organics include: hydrophobicity of the solute, organic carbon content and surface area of the sorbent. In the literature, peat and peat moss have received much attention as an amendment for creosote wastes (Rasmussen, G. et al. 2002; Yerushalmi, L. et al., 1999).

Peat-sand columns were used to treat creosote wastewater (Rasmussen, G. et al. 2002). They used 0.9% peat moss and achieved 94-100% removal of PAHs (slightly better removal with bioactive columns than abiotic columns). The majority of PAH removal was by sorption; however degradation could extend the life of a barrier, especially if PAHs that bind to the peat are still available for degradation. There was no apparent lag time before degradation started, and anaerobic degradation may also have been occurring in the columns (Rasmussen, G. et al. 2002). The authors suggest a two zone treatment method, where an initial zone would contain sand only and rely on biodegradation for removal, and a second zone containing peat would use sorption to remove any compounds that passed the bioactive zone (Rasmussen, G. et al. 2002). Other studies have demonstrated aerobic naphthalene degradation in sand columns (Warith, M., et al., 1998). Experiments using the solid phase microextraction (SPME) technique could provide a more detailed understanding of the high molecular weight PAHs in biologically active capping material. Column experiments have also been conducted to observe the migration of PAHs from freshwater sediment through Ottawa sand caps under advective conditions (Hyun, S. et al. 2006). Hyun et al. observed rapid breakthrough of PAHs in capping material, but when combined with oxic microbial processes, the flux of PAHs could be greatly reduced. These experiments were relatively short and did not account for sediment PAH dissolution. The addition of carbon amendments to the cap was not investigated.

The presence of an in situ cap shifts the location of depositional organic matter and removes the source of nutrients to the sediment (Himmelheber, D.W., et al. 2007). The lack of nutrients, in addition to anoxic conditions, could slow degradation at the sediment-cap interface (Hyun et al. 2006). Some types of organic additions to the cap could alleviate nutrients as a rate limiting factor. Ideally carbon amendments could slow the advective transfer enough to prevent contamination of the benthic zone pore water and surface water, while natural attenuation processes occur in the sediment and cap (Zimmerman, J.R. et al., 2004). Sorption to different forms of organic carbon has not been incorporated into cap designs. Generally sand has been found to be the easiest material to place as a cap and provides the greatest stability on sloped areas (Palermo, Clausner et al., 1998). Different forms of organic carbon could be used in the cap as an amendment. Equilibrium partitioning to the carbon can be used in modeling

approaches. However, the assumption of equilibrium needs to be examined in the sediment and cap. Particularly in the capping layers if pore water velocities are high and/or if inaccessible micro or macro pores exist in the cap. Standard published equilibrium partitioning values may be inadequate because of non-equilibrium conditions or competition effects between the hundreds of compounds found in the creosote and other non-aqueous phase liquids (NAPLs). Ultimately, a capping model may need to incorporate rate-limiting sorption processes by not assuming linear sorption equilibrium. This approach may provide better results when applied to long term modeling on low sorptive capacity sands with low organic content (Schuth, Ch. and Grothwahl, P. et al. 1994; Deane G., et al. 1999; Ran Y., et al. 2005).

IV. Materials and Methods

i) Sediment and column materials. Sediment and clean capping material (sandy gravel) from a representative portion of the cap where freshwater seepage was found occurring, was collected from the Wyckoff/Eagle Harbor, Washington Superfund site in June 2006 and stored at 4°C. The sediment collection effort was conducted as part of a related SERDP project (ER-1370). A detailed description of the source of the capping material is provided in the final report of the field activity portion of the project: ER-1370 (Sass et al., 2009). The material used in the columns was a sandy-gravel obtained from the existing cap in the field. It is representative of the material at the near/on shore areas where groundwater upwelling is most likely occurring (as determined by measuring pore water conductivity/freshening). The offshore Eagle Harbor cap is made of both Snohomish River dredge material (primary cap placed in 1993) and quarry-run sand placed as a secondary cap closer to shore in 2000. (Lyons et al. 2006, Myers et al. 2008).

The contaminated sediment used in this study was obtained by coring under the cap. There was a clayey (highly contaminated sediment) and a sandy (low contaminated sediment). The clayey sediment was obtained from TR5+20B, TR5+20A, TR5-00A, TR4+20A, and TR4+40A cores. The sandy sediment was obtained from TR4-00B and TR5-00A (see Figure 4-2 in Sass et al., 2009). The sandy and clayey sediment were mixed at a ratio 4:1 and then wet sieved to between 180 and 1700µm to obtain the contaminated source material used in the laboratory experiments. This sieve size was chosen because it was a size range in the fractional analysis of the bulk Eagle Harbor sediment that prevented excessive backpressure in the column experiments. It is important to remember that the purpose of the laboratory column experiments were to observe the generic behavior of PAH transport through capping material obtained from the field. The objective was not to replicate site specific source material and conditions at unique locations within the Eagle Harbor Superfund area.

Coal based granular activated carbon (45-180 µm) was obtained from Calgon Corp. (Pittsburgh, PA). Enriched Canadian sphagnum peat moss was obtained from Miracle-Gro Lawn Products, Inc. (Marysville, OH). The peat moss was ground and sieved to 63-1000 µm before being used as an organic carbon amendment. The peat moss was 30.9 % organic carbon. Total organic carbon (TOC) was measured using hydrochloric acid (HCl) pretreatment to remove inorganic carbon and combustion followed by nondispersive infrared (NDIR) detection of CO₂ in a Shimadzu TOC analyzer (Model TOC-5000A/SSM-5000A).

Initial sediment PAH characterization was done for the Eagle Harbor sediment and cap samples. The sediment and cap samples were homogenized and stored under refrigeration after it was received. Two

grab samples were taken and two portions (~2 grams wet weight) were taken for extractions from each grab. Extraction and analysis of sediment/cap material used pesticide-grade organic solvents obtained from Fisher Scientific (Pittsburgh, PA). The 16 EPA priority pollutant PAHs were measured in the sediment samples after ultrasonic extraction (EPA method 3550B) and silica gel cleanup (EPA method 3630C). Calibration standards were used at seven levels ranging from 103 to 31,000 µg/L of total 16 PAHs. Two internal standards, 1-floronaphthalene and p-terhpenyl-d¹⁴, were added to the GC vials prior to injection. Blanks and mid range calibration standards were run with samples to check background PAH levels and the initial calibration respectively. For PAH distribution by particle size, wet sieving was performed on the Eagle Harbor sediments using standard sieve sizes 63µm (mesh #230), 180µm (mesh #80), and 1.7mm (mesh #12). PAH extractions and analysis were performed for each of these sieved portions. Along with wet sample extraction, dry weights of sediment and cap samples were obtained from a portion (~5 grams wet weight) of each grab after overnight drying at 105 °C.

ii) Solid-Phase Micro Extraction (SPME) for PAH measurements. Ten parent PAHs were measured by solid phase microextraction (SPME) with gas chromatography mass spectrometry (GC-MS) in selected ion monitoring mode (Hawthorne, S.B., et al. 2005). SPME analysis procedure used commercially available 7 µm diameter PDMS [poly(dimethylsiloxane)] coated fibers from Supelco (Bellefonte, PA). A four point calibration was run using deuterated internal standards: naphthalene-d8, acenaphthylene-d10, flourene-d10, phenanthrene-d10, fluoranthene-d10, pyrene-d10 and chrysene-d12. The fiber was cleaned under a helium stream for 30 minutes at 320°C prior to running a set of samples. The fiber was cleaned for 10 minutes under a helium stream at 320°C between each sample run. Further details on the SPME method can be found in Hawthorne et al., 2005 (also in US EPA Method 8272). To verify the SPME technique used for sediment batch experiments, liquid-liquid extraction with hexane was also performed.

iii) Batch equilibrium measurements. For sediment equilibrium tests, a known mass (~ 1 g) of sieved sediment (180-1700 µm) was placed into each of six 11.5 ml glass vials with a solution of 0.01 M calcium chloride (CaCl₂) and 1000 mg/L sodium azide (NaN₃) in deionized water and capped with Teflon-lined caps. Vials were placed flat in a cylindrical container and on a roller for 16 days at 0.75 revolutions per minute (RPM). The equilibrated slurry was centrifuged at 4000 RPM for 6 minutes to produce 9 mL of aqueous supernatant from each sample vial that was transferred to new glass vials. Colloids were removed by flocculation by the addition of 0.25 ml of alum (10%wt) and 2 drops of 1N NaOH.

For capping material equilibrium tests, 3 grams of capping material was placed in 60 ml vials, and then filled with a 1000 mg/L NaN_3 solution. Capping material that had been baked in an oven at 70 degrees for four hours and capping material that had been baked at 400 degrees C for 4 hours were each used in the batch experiments making two forms of the capping material to be tested (baking at 400 degrees is assumed to remove labile organic carbon). Incremental amounts of PAH standards in acetone solvent were added to 7 vials for each form of the capping material to make a total of 14 vials. To one vial no PAHs were added to measure any PAHs desorbing from the clean capping material. To other vials with no capping material PAHs were spiked to check for losses to the vial cap and glass side walls. The vials were placed on a roller for 14 days after which time the water phase was measured for PAHs using SPME after alum flocculation.

For the peat moss equilibrium tests, approximately 0.1 grams for peat moss was placed in five 250 ml jars and filled with 1000 mg/L NaN_3 solution. Incremental amounts of PAHs were added to these five jars and five additional jars that didn't contain peat moss. Equilibration times were 3 weeks. Sorption to the vial glass and vial cap was assumed to be negligible in the presence of the sorbents.

iv) PAH Analysis by Gas Chromatography-Mass Spectrometry (GC-MS). PAH extraction of Eagle Harbor sediments and capping material was carried out using sonication with a hexane/acetone (1:1) mixture (based on EPA method 3550B for extraction). Clean-up on the final extract was carried out using an activated silica gel column as outlined in EPA Method 3630C. A gas chromatograph (Agilent model 6890N) with a 0.25- μm bonded fused silica capillary column (DB-5MS, 60 m x 0.25 mm i.d.) coupled with a mass spectrometer (Agilent model 5973 Network Mass Selective Detector) was used for analysis based on EPA method 8270C for 16 parent PAHs.

An initial ultrasonic extraction with acetone followed by a mixture of hexane/acetone (1:1) was used to extract the creosote from the sieved Eagle Harbor sediment. The mass of the total extractable organics was determined gravimetrically by evaporating the solvent from the extract under a steady air stream (similar to EPA Method 9071A).

v) Column studies. Column experiments were conducted in 5 cm diameter glass columns with 6 equally spaced Teflon sampling ports as illustrated in Figure 1. Glass wool separated the sampling ports from the sediment and capping material. Port 1 was positioned at the sediment layer and sampled sediment pore water, ports 2-5 were positioned at the capping layers and port 6 was positioned at the overlying water. The sediment was sieved to 180-1700 μm prior to being used in columns to allow for desired flow rates to occur without creating excessive backpressure. Sieving the sediment decreased the total 16 PAH

concentration from 1162 to 850 $\mu\text{g/g}$. The sediment was placed in the column from the top using a PVC pipe to prevent pre-contamination of the glass side walls. The flow was maintained at 25 ± 5 mL/hr for specific discharge rates (i.e. Darcy velocity) of approximately 0.015 m/h (which is likely 15 times greater than at Eagle Harbor site) and average pore water velocities of 0.05 m/hr. These conditions provide a Reynolds number of 0.0004 which is well below 0.01 to be considered laminar flow. The flow direction was up through a 14 cm deep sediment layer, a 65 cm capping material layer, and 32 cm of overlying water. The sediment and capping material did not compress and these distances remained constant during the length of the experiment, and porosity was assumed to be constant as a function of depth. Three of the four columns were constructed with amendments in the capping material. All columns were run with the influent water containing 0.01M CaCl_2 to mimic the ionic strength of groundwater (this conductivity is about 13 times less than the pore water of the capping material as shipped) and 100 mg/L NaN_3 (to inhibit microbial activity) in abiotic columns. Ten parent PAHs were measured in pore water samples by SPME GC-MS as described previously. The five column experiments that were run were as follows:

1. killed control column with no amendment to the capping material.
2. killed column with capping material amended with 2% GAC
3. killed column with capping material amended with 0.2% TOC by the addition of peat.
4. killed column with capping material amended with 0.2% GAC
5. biologically active column with no amendments in the cap.

The percent amendment added is by weight. The amendments were mixed in the capping material prior to addition to the columns. The mass-median diameter (D_{50}) values for the GAC and peat amendment were $110\mu\text{m}$ and $530\mu\text{m}$ respectively. The D_{50} value for capping material was 2.75mm.

The flow through the columns was measured by collecting effluent water in a graduated cylinder. The flow was generally 26ml/hr but may have increased to 30ml/hr at times. As a rule of thumb, when the column diameter to particle diameter ratio is greater than 20, the side wall effects are considered to be negligible. Our columns had a column to particle diameter ratio of 18.5, close to the ratio suggested for no wall effects. Tracer studies conducted in the columns packed with capping material show normal Gaussian shape of the tracer and no indication of significant wall effects. Short circuiting would result in fronting of the Gaussian curve, but this is not visible in the tracer results. If glass side walls were of major significance they would have allowed premature breakthrough in the amended columns. This was not observed either as discussed in the later part of the report.

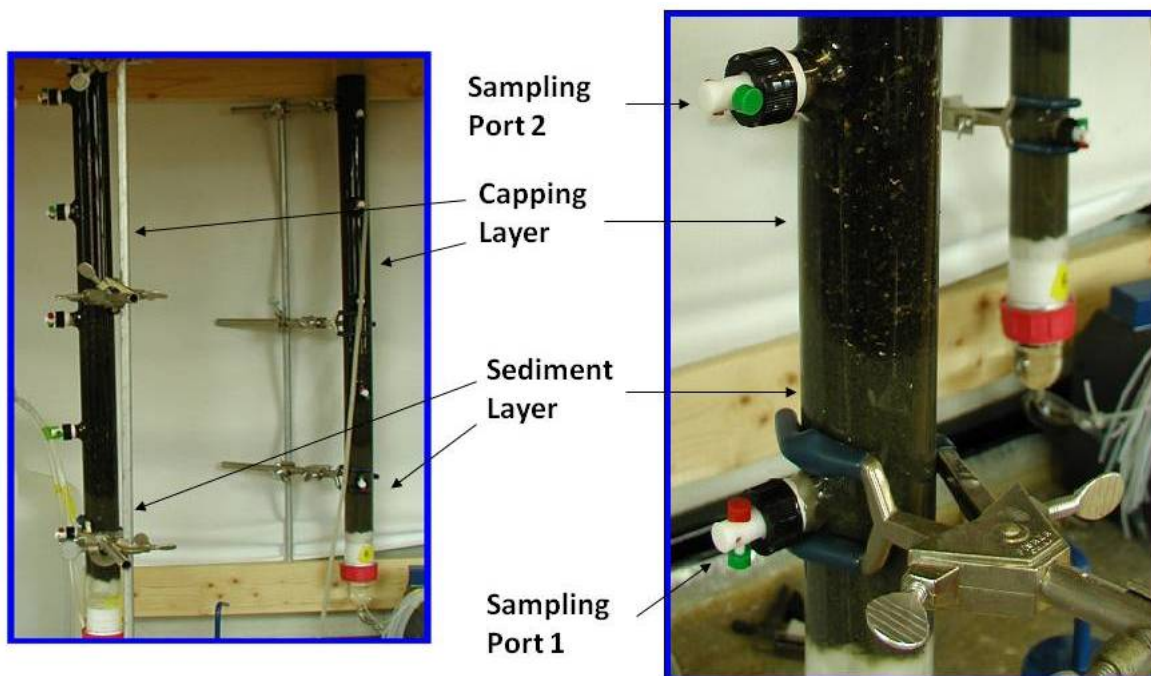
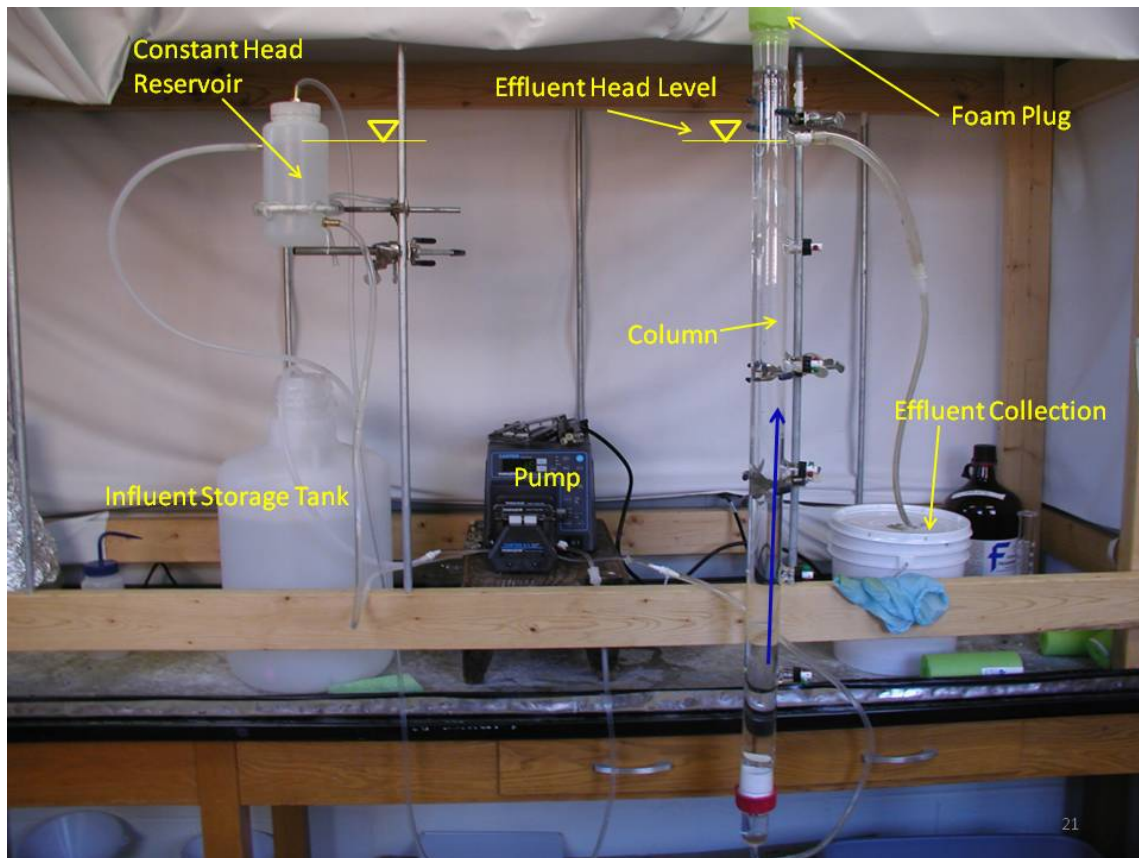


Figure 1. Pictures of laboratory column setup showing plumbing setup (top) and closeup of sampling ports (bottom)

vi) Modeling contaminant transport . The dissolution of PAHs from multi-component NAPLs (such as creosote) has been modeled previously (Peters, C., et al., 1999). This system more adequately describes the sediment found at many PAH contaminated sites with high concentrations of free phase creosote or coal tar (Hong L. et al., 2003). The modeling utilizes ordinary differential equations describing the mass balances in the creosote and water phases of the modeled porous media. A sediment particle that is coated with a thin layer of creosote can be modeled using Raoult's law and coupled mass balance equations for creosote, aqueous, and solid phases. The mass balance for PAH i in the aqueous phase is

$$\frac{dC_i^A}{dt} = k_{ai}(C_i^* - C_i^A) - \frac{C_i^A}{\tau} - k_{bi}C_i^A \quad \text{equation 1.}$$

where C_i^A is the concentration of i in the aqueous phase (mg/L), k_{ai} is a mass transfer rate constant (t^{-1}), C_i^* is the aqueous phase solubility (mg/L), τ is the aqueous phase residence time (t), and k_{bi} is the biodegradation rate constant, (t^{-1}). The solubility is related to creosote composition through Raoult's law

$$C_i^* = X_i^N S_i \quad \text{equation 2.}$$

where X_i^N is the mole fraction of i in the creosote phase, and S_i is the subcooled liquid solubility for i . The mass balance for i in the creosote phase is

$$W_i \frac{dm_i^C}{dt} = -k_{ai}V^A (C_i^* - C_i^A) - P_i \quad \text{equation 3.}$$

where W_i is the molecular weight of i (g/mol), m_i^C is the moles of i in the creosote phase (mol), V^A is the volume of the aqueous phase (L^3), and P_i is the rate of precipitation (or redissolution) of i . The mass balance of the solid PAH phase is

$$W_i \frac{dm_i^S}{dt} = P_i \quad \text{equation 4.}$$

where m_i^S is the moles of solid i (mol). Assuming the creosote and solid phases are in equilibrium, solid PAH will begin to form when the PAH's mole fraction reaches its solubility limit in the creosote phase. Solubility limits as well as other properties of PAHs are listed by Peters et al. A conceptual schematic for this model is shown Figure 2.

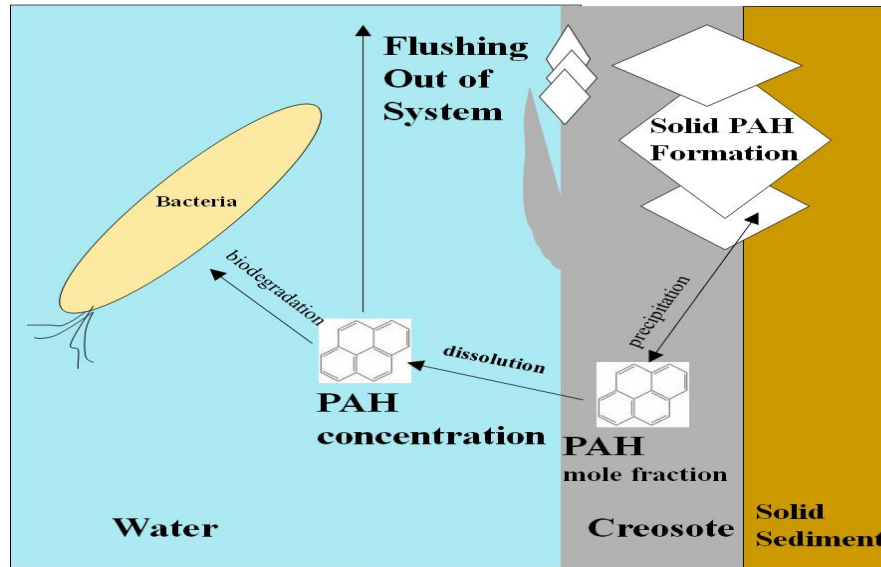


Figure 2. Conceptual model schematic for PAH dissolution from creosote contaminated sediment.

Discrepancies in the sediment dissolution model could be explained by the mass transfer rate which assumes homogeneous creosote/water surface area throughout the control volume. In reality, the creosote/water surface area will be least at the inlet end of the column and will increase as the dissolution front is reached (Imhoff, P.T. et al. 1993). The model may fail to describe the creosote/water mass transfer changes if solid PAH formation occurs at the creosote/water interface (Luthy, R.G., et al., 1993; Ortiz, E. et al. 1999). The model assumes equilibrium between the solid and creosote phases.

Experimental results of a biologically active column can be compared to the model to see if the mass transfer of PAHs from the sorbed phase to the aqueous phase controls biodegradation rates. Errors in the model could also arise from microbial utilization of sorbed and creosote phase PAHs (Xia, X. et al. 2007).

The migration of a single contaminant in a sediment cap has been described using the one dimensional advection-dispersion equations with retardation for steady state flow in homogenous soil. (Toride et. al. 1999).

$$R \frac{\partial Cr}{\partial t} = D \frac{\partial^2 Cr}{\partial x^2} - v \frac{\partial Cr}{\partial x} - k_b Cr \quad \text{equation 5.}$$

where Cr is the volume averaged or resident concentration ($\mu\text{g/L}$) of one particular PAH in the column, D is the dispersion coefficient (m^2/day) obtained by tracer studies of capping material columns, v is the average pore-water velocity and R is a retardation factor given by

$$R = 1 + \frac{\rho_b K_d}{n} \quad \text{equation 7.}$$

where ρ_b is the cap solid bulk density (kg/L), K_d is the solid-water distribution coefficient ($\mu\text{g}/\text{kg}/\mu\text{g}/\text{L}$), and n is porosity. The distribution coefficient depends on the properties of the capping material and assumes equilibrium partitioning in the cap:

$$K_d = K_{d\text{cap}} + f_{oc} * K_{oc} + f_{ac} * K_{GAC} \quad \text{equation 9.}$$

where $K_{d\text{cap}}$ is the solid-water distribution coefficient of non-amended cap, f is the fraction of organic carbon (OC) or granular activated carbon (GAC), K_{oc} and K_{GAC} are the distribution coefficients for OC and GAC respectively. Analytical solutions to the advection-dispersion equation with retardation (Ogata, A. and Banks, R.B., 1961), but without biodegradation, have been utilized for preliminary calculations

$$C = \frac{C_0}{2} \left[\text{erfc} \left(\frac{x - \left(\frac{v}{R}\right)t}{2\sqrt{\left(\frac{D}{R}\right)t}} \right) + \exp\left(\frac{vx}{D}\right) \text{erfc} \left(\frac{x + \left(\frac{v}{R}\right)t}{2\sqrt{\left(\frac{D}{R}\right)t}} \right) \text{erfc} \left(\frac{x + \left(\frac{v}{R}\right)t}{2\sqrt{\left(\frac{D}{R}\right)t}} \right) \right] \quad \text{equation 10.}$$

where C is the PAH concentration ($\mu\text{g}/\text{L}$) of the column effluent, C_0 is the PAH concentration ($\mu\text{g}/\text{L}$) of the column influent, and x is the distance along the column. A numerical simulation (using CXTFIT code) of equation 5 provides the ability to incorporate a changing boundary condition to the cap, biodegradation in the cap, and initial porewater concentrations in the cap.

vii) Numerical solution for the NAPL dissolution model

A mathematical model described by the equations presented in the previous section was coded in MATLAB software (where the creosote phase is labeled as non-aqueous phase liquid (NAPL)). A mass transfer coefficient (days^{-1}) is used to characterize the migration of PAHs from the creosote phase to the water phase (Imhoff, P.T. et al., 1993). A variable (`m_napl_init_total`) is set at 0, and is used to calculate the initial amount of moles of PAHs in the system. A variable (`m_napl_total`) is also set at zero and is used for updating the total amount of moles after each time-step. Arrays are declared for the moles and the mole fraction of PAH i in the creosote, the PAH concentration in the aqueous phase, and the solubilities of the PAHs in the creosote. Properties pertaining to each PAH were imported from an excel

file as initializers. The initializers used were as follows: the PAH name, molecular weight, biodegradation rate, initial mole fraction, subcooled liquid solubility, and initial moles. A time array is used to fill out where the initial element is, (initial time) and ends at the maximum number of time points incrementing by the given time step (dt) in each element using a 'for-loop'. Two 'for-loops' follow this; the first is used to calculate the moles of creosote using equation 3 and sums the initial total amount of moles of creosote for each compound for that time step. If the mole fraction in the creosote phase is greater than the solubility limit of that PAH in the creosote phase then a precipitation rate is calculated and the moles in the solid phase are calculated using equation 4. The mole fraction in the creosote phase is then set to the solubility limit and the aqueous phase solubility is set using equation 2. The moles of solid PAH are tabulated. The condition when the mole fraction of the PAH in the NAPL phase is less than the solubility limit (and solid PAH is present) is checked for. If this condition occurs, a redissolution rate is calculated and moles of PAH in the solid phase is calculated using equation 4. Again, the new solubility limit is set using equation 2 and the moles of solid PAH is tabulated. Finally, the concentration of PAH in the aqueous phase is calculated numerically using equation 1. The basic algorithm structure (just described) is provided in the appendix.

V. Results and Accomplishments

i) Characterization of sediment and capping materials. The total concentration for 16 EPA priority pollutant PAHs in the Eagle Harbor Sediment was $1162 \pm 108 \mu\text{g/g}$. The individual PAH concentrations for bulk sediment and cap material are shown in Figure 3. The 2-3 ring PAHs dominated the distribution in Eagle Harbor sediment. The total PAH concentration in cap material was lower by four orders of magnitude ($0.098 \pm 0.012 \mu\text{g/g}$). The PAH distribution in the cap material was different with more higher molecular weight PAHs present compared to the Eagle Harbor sediments. The Eagle Harbor sediment TOC was found to be $0.31 \pm 0.01 \%$ by weight. The low TOC and high PAH content of sediment raises an interesting observation that a majority of the TOC may be contributed by PAHs. The 16 priority pollutant PAHs comprise nearly a third of the sediment TOC. For tar-impacted manufactured gas plant sites, Hawthorne et al (2006) showed that the priority pollutant PAHs comprise about 40% of the total PAHs including the major alkylated homologs (a total of 34 PAHs). Thus, it appears that nearly all of the TOC may be explained by the contribution from parent and alkylated PAH compounds that may be present in the Eagle Harbor sediment. This observation may indicate the lack of an organic matter sorption phase in the sediment. In the absence of a sorbent organic matter phase, the PAH mixture may be present as a separate oil phase that coats the sediment inorganic particles, much like what may be expected from a creosote-contaminated sediment. Additional evidence of a creosote coating on particles is seen in the data for PAH distribution by particle size class. The distribution of PAHs in different size fractions of the Eagle harbor sediment and cap are shown in Table 1. As shown in Table 1, the PAH concentration is higher in the smaller particle sizes indicating a surface coating or surface adsorption phenomenon. The highest PAH concentration of 34,690 mg/kg is observed in the smallest particle size range (< 63 microns).

Table 1. PAH distribution in four size fractions of Eagle harbor sediment.

Grain size μm	Weight fraction %	Total PAH $\mu\text{g/g}$	PAH fraction % by total
> 1700	5	969	2
170 – 1700 *	77	846	32
63 - 170	15	2,039	15
< 63	3	34,690	51

* Used for column experiment; TOC content: $0.4 \pm 0.01 \%$ by wt

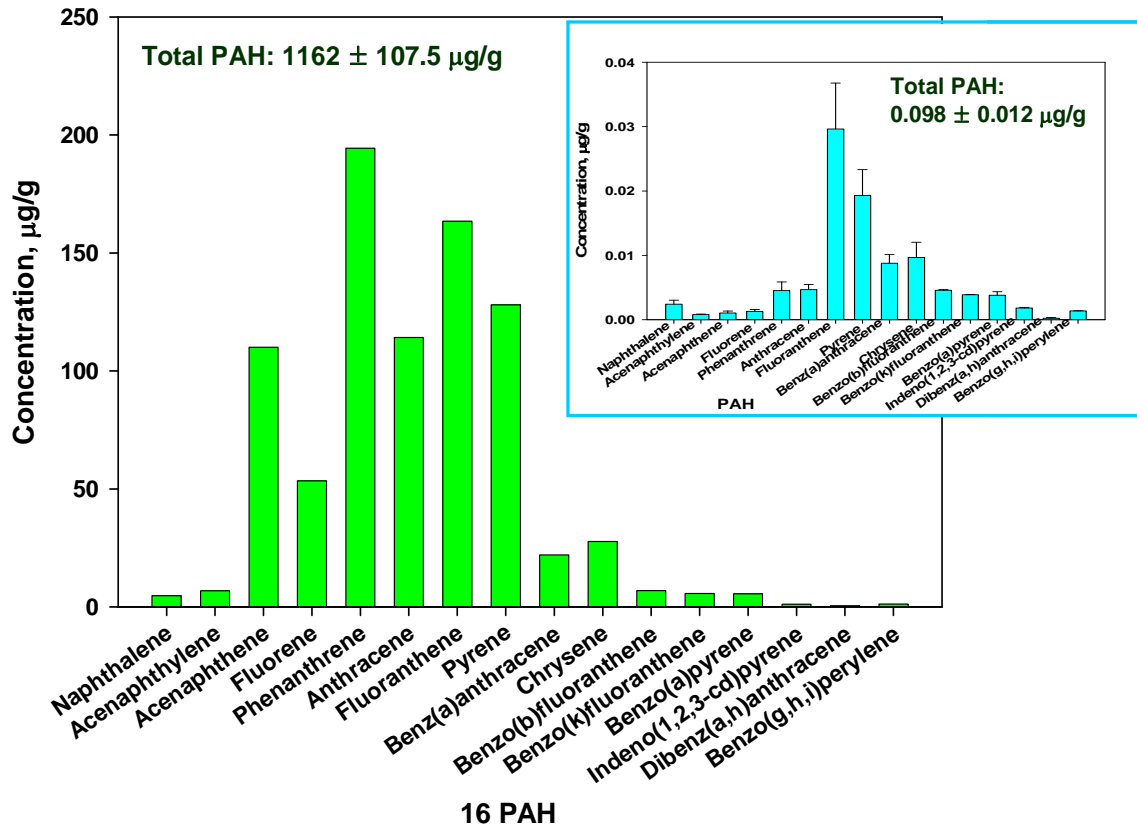


Figure 3. The individual PAH concentration for bulk sediment and cap material (inset)

A total of 16 EPA priority pollutant PAHs were measured to be 846 µg/g in the sieved Eagle Harbor sediment. PAHs such as acenaphthene, phenanthrene, anthracene, fluoranthene and pyrene appear dominant. The higher molecular weight PAHs (greater than chrysene) are found in continually decreasing concentrations which is characteristic of pyrogenic PAHs associated with distilled, coal-derived liquids such as creosote (Brenner, R.C. et al. 2002; Stout, S.A., et al., 2001). The TOC of the sediment was 0.40±0.01% by wt. The percent organic carbon in the sediment after PAH extraction was found to be 0.09%, indicating that the extractable material (mostly PAHs) accounted for 77.5% of the TOC in this sediment. This would indicate a creosote content of 0.3%. The creosote content of the sediment was measured to be 0.002 g/g (0.2%) using the hexane/acetone extractables method. Some lighter molecular weight PAHs may have been lost during evaporation of hexane/acetone in the extraction method. The capping material had low initial PAHs (0.098±0.01 µg/g) and TOC (0.04±0.01% by wt.). Both the sediment and capping material used in this study have extremely low levels of native organic carbon.

ii) Sediment-water equilibrium measurement. Batch equilibrium tests were conducted using whole and sieved sediment. Sieving was performed using U.S. standard sieve numbers 80 and 12 to collect material between 180 and 1700 μm . As shown in Figure 4, the whole and sieved sediments gave nearly identical aqueous PAH concentrations, which is expected based on the mechanism of a creosote phase coating the mineral surfaces. The most abundant PAH in the aqueous phase was acenaphthene followed by phenanthrene and fluorene. The concentration of PAHs larger than chrysene was barely detectable in the aqueous phase. As shown in Figure 5, the TOC normalized solid-water distribution ratios ($\log K_{\text{TOC}}$) ranged from 4.3 to 7.1 and generally agreed well with literature values for PAH impacted sediments taken from Cornelissen et al (2006), Cornelissen and Gustafsson (2004), and Jonkers and Koelmans (2005).

The measured $\log K_d$ values for sieved Eagle Harbor sediment, capping material, and peat moss amendment are shown in Table 2. The $\log K_d$ values of the sediment are low (ranging from 2.2- 4.4) primarily due to the low organic carbon content in sediment. For peat moss, the measured K_{oc} values are close to the predicted K_{oc} values based on the frequently used correlation by Karickhoff et al. (1979). In the capping material, organic carbon partitioning is low and plays a competing role for the sorption of PAHs with mineral surfaces. The expected K_d due to organic carbon in the capping material was first estimated using published organic carbon-water partitioning coefficients (K_{oc}) (Hawthorne et al. 2006) and the capping material organic carbon content of 0.04%. For example, the K_d for pyrene should be 16.3 L/Kg ($K_{\text{oc}} \times f_{\text{oc}} = 104.61 \times 0.0004$). In material that has a fraction of organic carbon (f_{oc}) less than about 0.001, sorption to mineral surfaces may play a significant role. This could lead to larger K_d values in batch experiments than would be expected by organic carbon fractions alone (Mader, B.T. et al. 1997). However, the K_d for pyrene in the capping material was measured to be only 6.10 ± 4.36 L/Kg. It is expected that less pyrene would be sorbing to the cap in these experiments because they were done with a mixture of 13 PAHs ranging from naphthalene to chrysene. Competition for sorption sites may occur in these batch experiments resulting in lower K_d values. When the capping material was heated at 400 °C for four hours, the K_d was 3.77 ± 1.50 L/Kg, indicating that labile (or amorphous) organic carbon contributed to some, but not all, of the sorption to the cap in these experiments. It has been theoretically demonstrated that at phenanthrene concentrations of 0.2 $\mu\text{g/L}$ or greater, sorption to carbonaceous geosorbents (such as kerogen) begins to be less important than amorphous organic carbon (ratio of CG to AOC; 1:10) (Cornelissen, G. et al., 2005). Longer sorption times in the batch experiments can result in higher sorption of PAHs due to the small and perhaps inaccessible organic carbon fraction trapped in micropores or macropores of the capping material. Others have found sorption and desorption times of months to years are possible for PAHs entrapped in the organic carbon of soil and sediment pores (Pignatello, J.J, 1990 and 1995; Schuth, Ch. and Grothwahl, P. et al. 1994; Ran Y. et al. 2005).

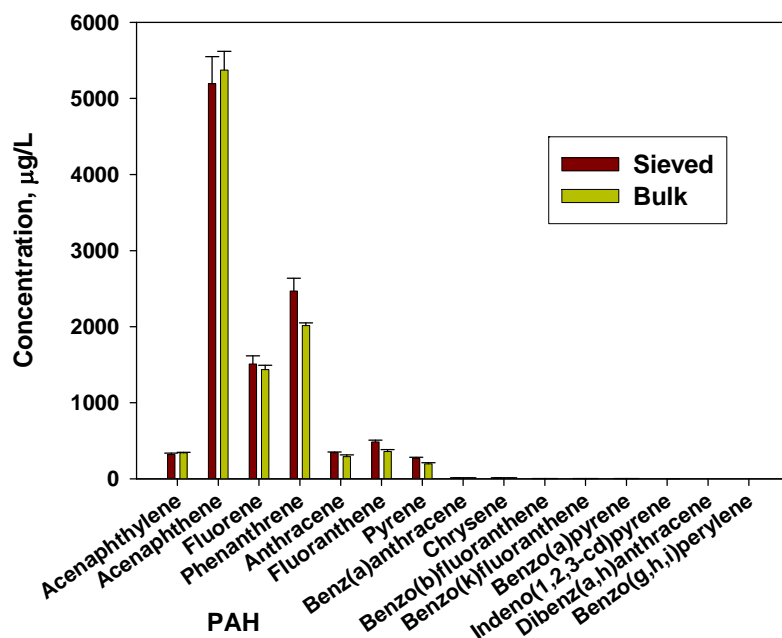


Figure 4. Equilibrium aqueous PAH concentration for bulk and sieved fraction of PAH contaminated Eagle Harbor sediment.

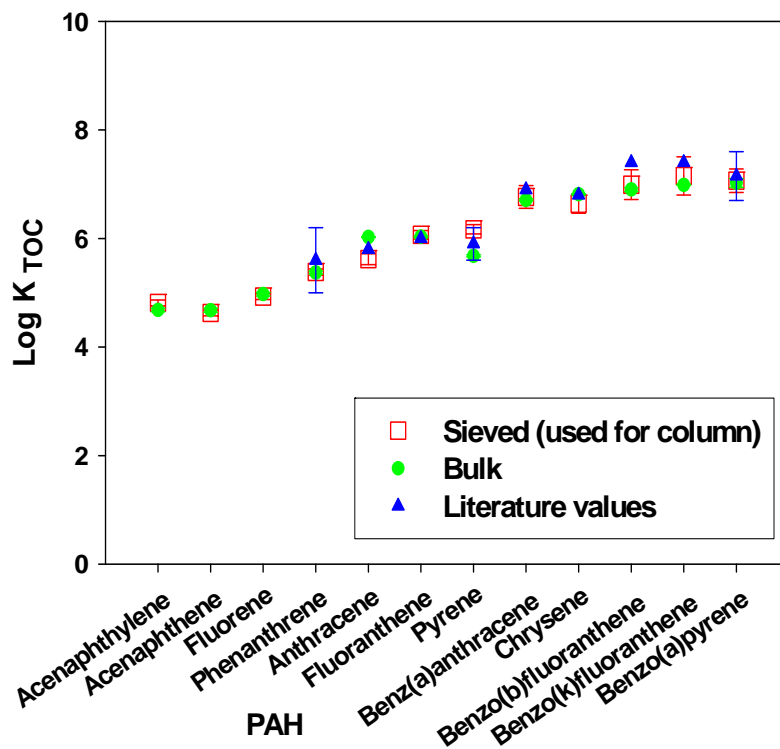


Figure 5. TOC normalized solid-water distribution ratios ($\log K_{TOC}$) of PAH

Table 2. Log K_d values for Sieved Eagle Harbor Sediment, capping material, and peat moss amendment.

PAH	Log K _d sediment	Log K _d cap	Log K _{oc} Peat Moss	Log K _{oc} (logK _{oc} = 0.63 logK _{ow})
Naphthalene	2.24±0.13	0.35±0.21	3.28±0.23	3.09
Acenaphthalene	2.21±0.07	0.28±0.19	2.66±0.42	3.73
Acenaphthene	2.03±0.07	0.23±0.18	2.79±0.32	3.71
Fluorene	2.30±0.05	0.30±0.15	3.45±0.11	3.97
Phenanthrene	2.82±0.03	0.64±0.07	3.95±0.08	4.25
Anthracene	3.40±0.05	1.48 ±0.39	4.37±0.18	4.24
Fluoranthene	3.49±0.03	1.41 ±0.13	4.56±0.30	4.74
Pyrene	3.63±0.03	1.38 ±0.09	3.84±0.11	4.67
Benz(a)anthracene	4.01±0.06	1.98 ±0.18	5.75±0.15	5.45
Chrysene	4.29±0.05	2.04 ±0.06	5.61±0.11	5.45

iii) Column studies without amendments. Column studies were conducted first without amendments to evaluate breakthrough of PAHs under advective conditions. Breakthrough is defined as the bed volumes (or time) at which effluent (port 6) concentrations are 50% of sediment pore water (port 1) concentrations (BT50). Figures 6 and 7 show data from a column with no amendments initially, and after 8 bed volumes have passed. Hollow symbols represent data below the limit of quantification (LOQ) or above the calibration range. Initially the PAHs were not distributed throughout the entire cap layer and then after 8 bed volumes the PAH concentrations went beyond the BT50 (breakthrough probably occurred between 5-8 bed volumes). Benz(a)anthracene and chrysene pore water concentrations still decreased along the length of the column after 8 bed volumes. This is due to their low water solubilities and higher sorption to solids relative to the other PAHs measured. Initially naphthalene appears at higher concentrations in the cap near the sediment (port 2) than in the sediment layer (port 1). This is possibly due to the migration of

naphthalene in porewater during column construction. During column construction, PAHs such as naphthalene reside in sediment porewater and small amounts of water overlying the sediment. Sediment porewater and sediment overlying water becomes incorporated in the pore water in the capping material closest to the sediment, carrying PAHs to lower levels in the cap (ports 2 and 3). As seen in Figures 6a, there appears to be little retardation of PAHs in the column. Even the expressed water during cap placement transports low molecular weight PAHs nearly half way through the cap in the column. After 8 bed volumes all the PAHs have broken through the sand cap (Figure 6b). Naphthalene is seen to be depleting in the sediment layer (port 1) likely due to the higher aqueous solubility and mobility of this compound. Other low molecular weight PAHs appear to deplete during the length of the experiment because they are readily released from the creosote phase, while high molecular weight PAHs such as pyrene, benz(a)anthracene, and chrysene continue to increase in the sediment pore water throughout the length of the experiment.

Based on these experiments, it appears that measuring pore water concentrations is critical in determining breakthrough of PAHs in a cap. When solid phase PAH concentrations are used, the degree of pore water transport could be underestimated in cases where the cap has low sorption capacity. Based on the low K_d values of the capping material (Table 2), very little of the PAHs are expected to adhere to the cap. The expected PAH concentration in the capping material was calculated based on the measured K_d values for the cap and porewater concentrations. Also, at the end of the column experiment, the column contents were frozen in dry ice and sectioned for PAH extraction and measurement. The results of PAH measurement in cores taken out of the cap in the field is compared with measurements from the laboratory column and modeling predictions in Figure 7. The results are presented as total PAH concentration profile as a function of distance from the sediment-cap interface. The PAH concentrations in the field cap range from 0-20,000 $\mu\text{g}/\text{kg}$, with the higher concentrations near the sediment-cap interface. These concentrations seen in the cap can be considered close to the background levels of PAHs often found at harbor sites (Magar, V.S. et al., 2007). The measurement of 16 PAHs obtained from the laboratory experimental column compared well with PAH measurements from field cap cores (Figure 7). The modeling predictions based on the partitioning between porewater and cap material also is in the range of measured values in the field and laboratory. A key conclusion of this comparison is that measurement of PAH concentration in cores taken out of sediment caps is a poor indicator of contaminant breakthrough, especially in cases where there is little capacity in the cap material to sorb contaminants. In-situ porewater concentrations need to be measured to provide an assessment of contaminant movement through caps.

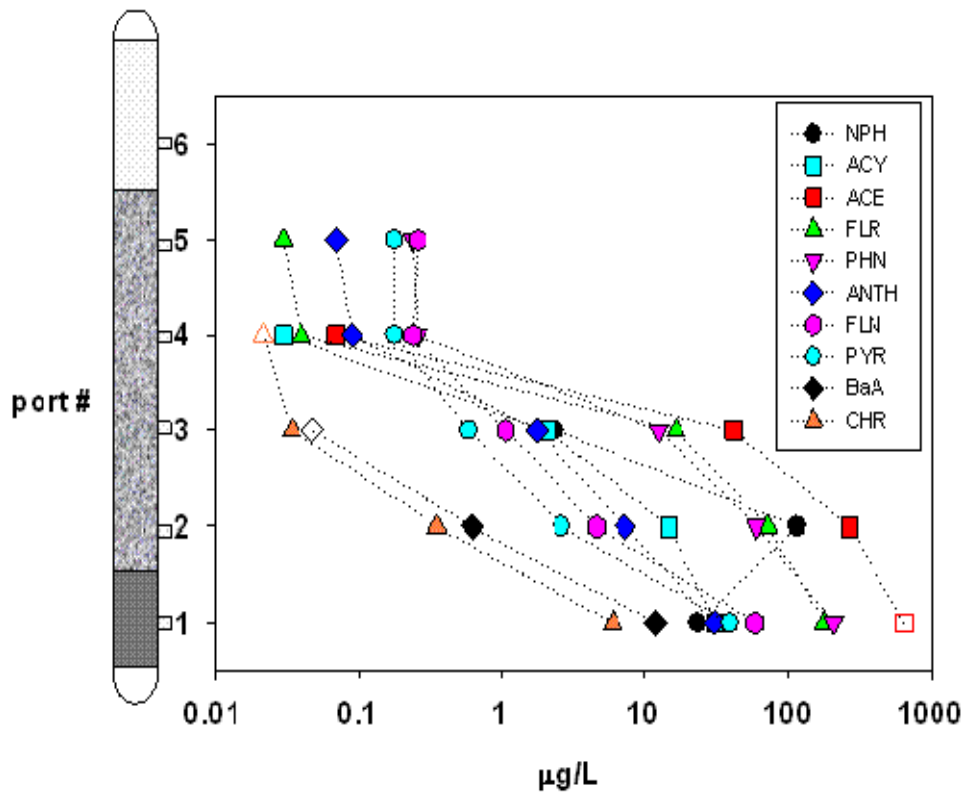


Figure 6a. Initial PAH distribution in sediment and cap without amendments

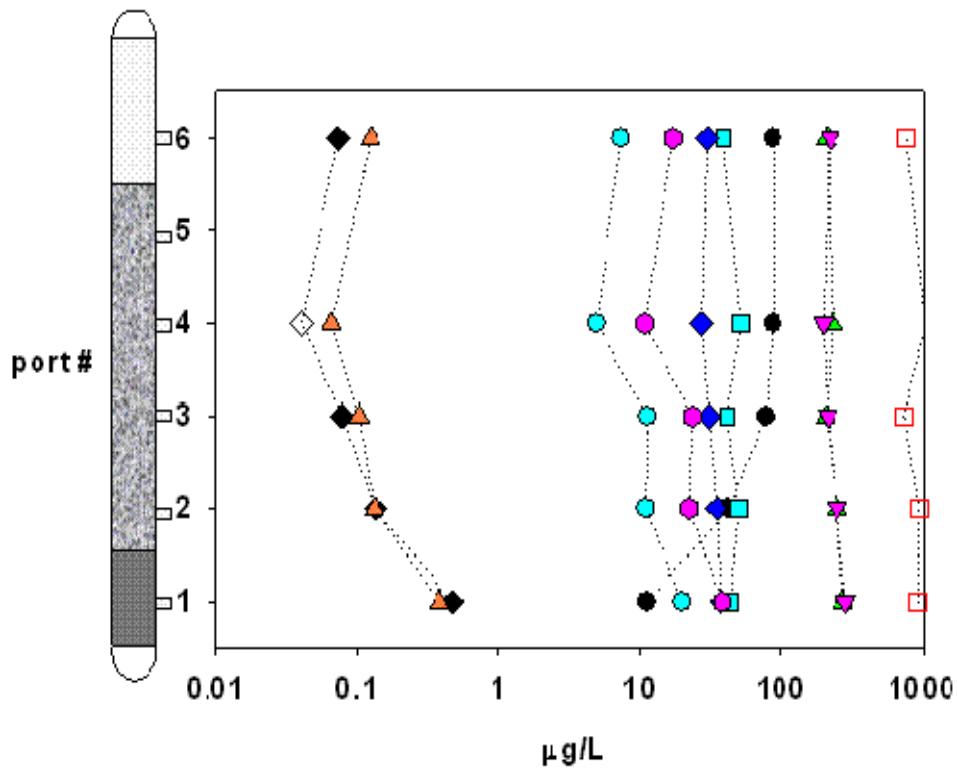


Figure 6b. PAH Breakthrough after 8 bed volumes in a cap with no amendments.

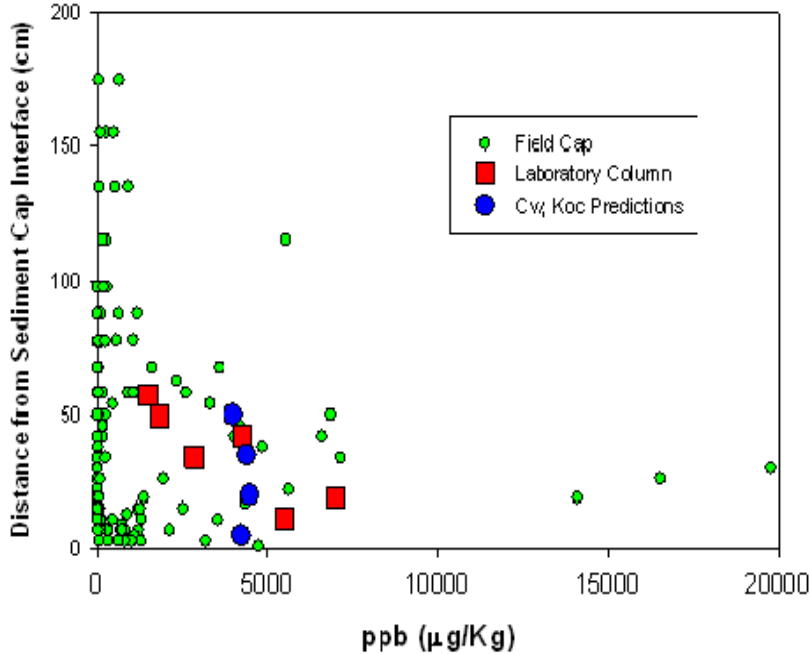


Figure 7. PAH measurements in a field cap (Sass et al., 2009) compared to measurements in a laboratory column and theoretical predictions.

iv) Column studies with amended caps

Peat moss amendment. Column studies with amendments were conducted to explore the potential retardation of PAH migration in the cap. Columns with 2% TOC amendment in the form of peat moss created a lot of backpressure and flow rates of 25 ml/hr could not be achieved. In a column with 0.2% TOC amendment, adequate flow rates could be maintained and a delayed breakthrough of PAHs occurred (Figure 8). Slight turbidity was observed (3.3 NTUs) initially in the column effluent, but reduced to 1.4 NTUs within a week. This level of turbidity is not expected to correspond to dissolved organic matter levels that would affect the SPME measurement. SPME fibers have been used to measure PAHs in dark brown coal wastewater with DOM concentrations as high as 350 mg/L (Poerschmann, J., et al., 1998). The migration of PAHs in a column amended with 0.2% TOC was slower than that observed in columns with no amendment. Breakthrough of naphthalene was observed after 6.2 bed volumes and other light PAHs after 46.5 bed volumes. Pyrene concentrations in porewater from port 4-6 remained an order of magnitude less than pore water concentrations from the sediment layer (port 1). Porewater concentrations of pyrene from the sediment layer continued to increase even after 150 bed volumes.

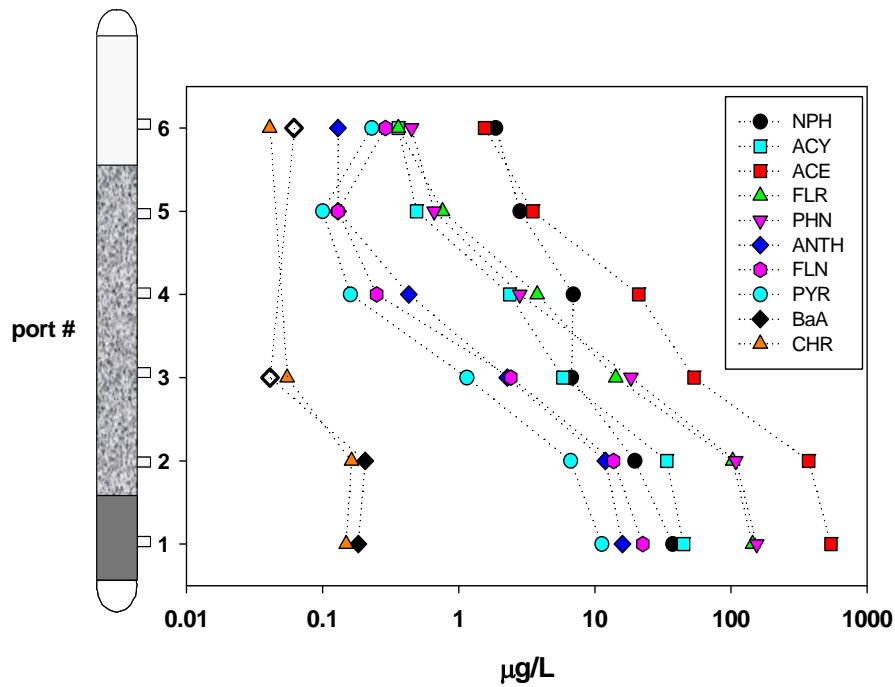


Figure 8a. Early PAH profile in a cap with peat moss amendment (1.9 bed volumes).

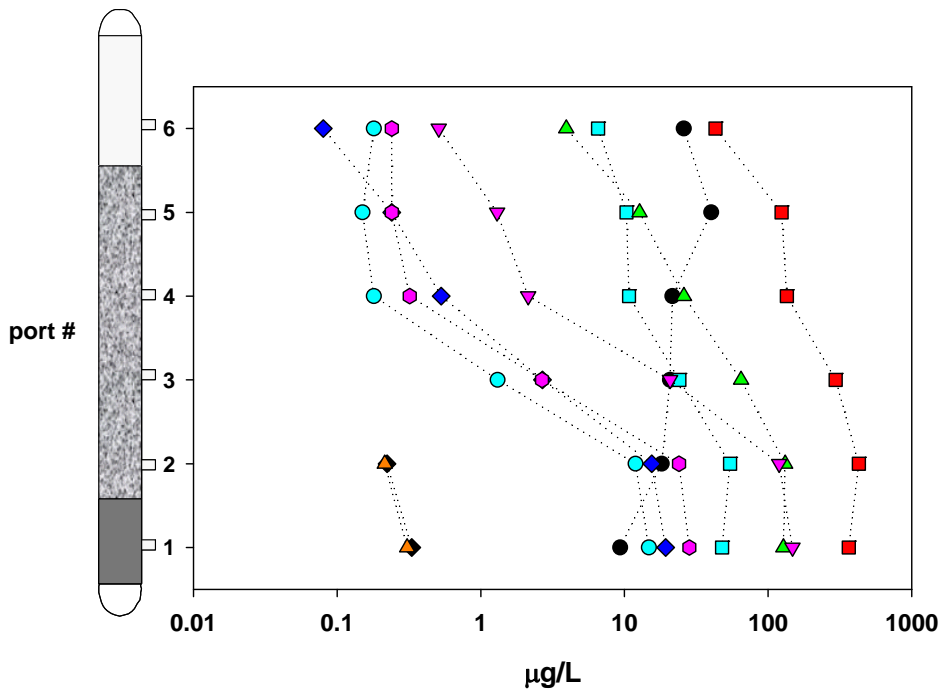


Figure 8b. PAH Breakthrough after 11.3 bed volumes in a cap with peat moss amendment.

Activated carbon amendment. Activated carbon (AC) at 0.2 and 2% dry weight was added to the capping material in separate columns. It can be seen that 2% GAC greatly reduced the transport of PAHs after 18 bed volumes (Figure 9). In 0.2%GAC amended columns, concentrations remain low in the capping material, however, they did reach detectable levels of the PAHs. The low molecular weight PAHs depleted faster from the sediment porewater for the 0.2%GAC column than in previous experiments, making the 2% GAC column a better comparison to the column with no amendment. With 2% AC, the capping material (ports 3-5) remained well below quantitation levels for the length of the experiment. High molecular weight PAHs were slightly above quantifiable levels in the capping material at port 2. This transport is most likely due to porewater PAH displacement during column construction (not due to sediment consolidation). PAH detection may also be attributed to the slower rate at which high molecular weight PAHs (e.g. pyrene) enter pores in the GAC relative to low molecular weight PAHs (e.g. naphthalene). Accessibility of pollutants to black carbon pore networks is dependent on pollutant molecular size (Zhu, D. et al., 2005).

Visually the water samples appeared to be clear for every column except for the initial samples from the column amended with peat moss. Solid phase microextraction using an internal calibration with deuterated (d-PAH) internal standards for each PAH measures total dissolved PAHs (freely dissolved and DOM associated) (Poerschmann, J. et al. 1997; Poerschmann, J. et al. 1998). However, at low turbidity (<1.4 NTU) for the PAHs measured, the DOM fraction is small relative to the freely dissolved concentration. Figure 9A-9H. show all the data for a middle and high molecular weight PAH (phenanthrene and chrysene) over many bed volumes at the sediment layer (port 1) and the overlying water (port 6) for each column. From these graphs it is apparent that GAC is an effective amendment, but that peat moss (0.2% TOC) was also somewhat effective for the high molecular weight PAHs (e.g. chrysene).

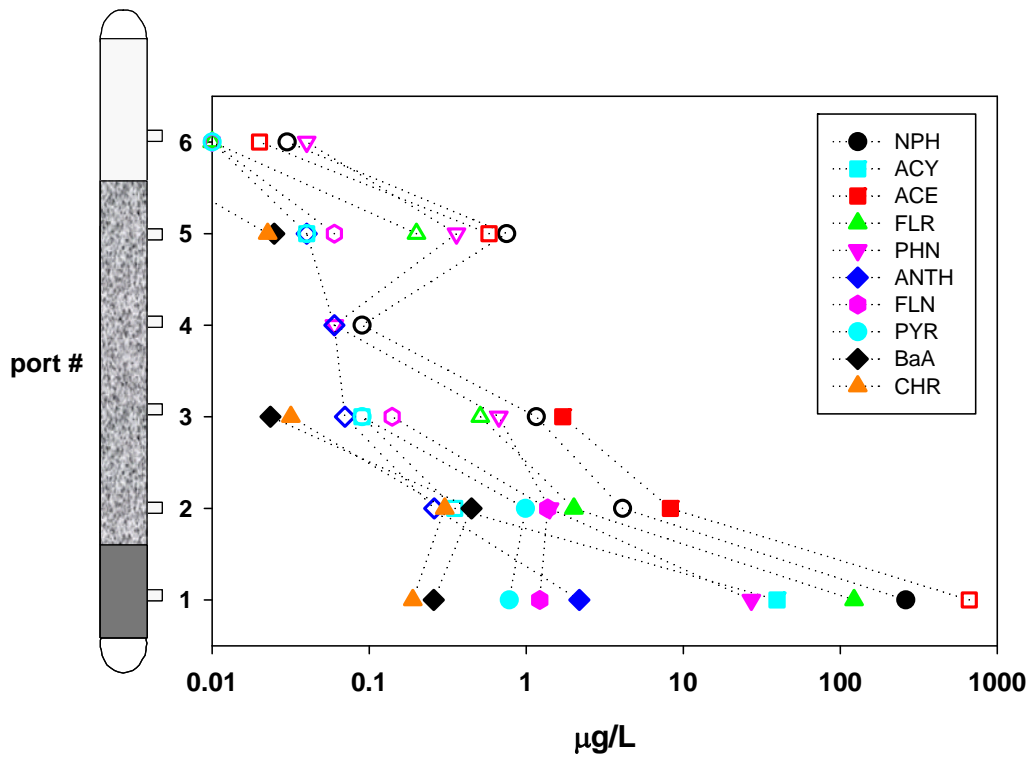


Figure 9a. Initial PAH profile in experimental cap amended with 2% activated carbon.

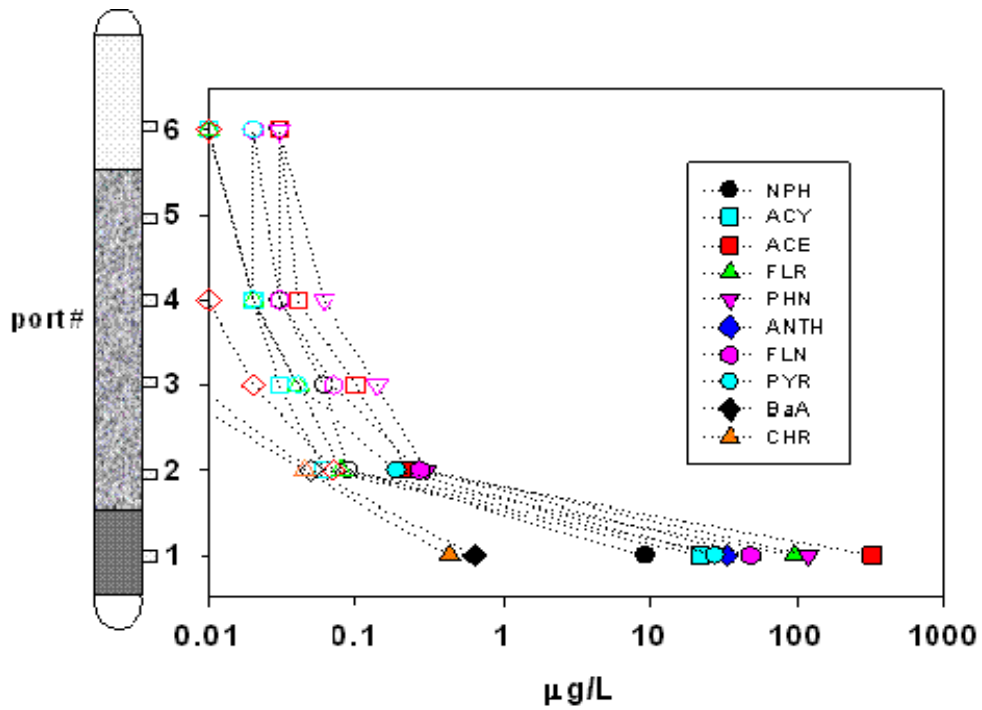


Figure 9b. PAH profile in experimental cap amended with 2% activated carbon after 18 bed volumes.

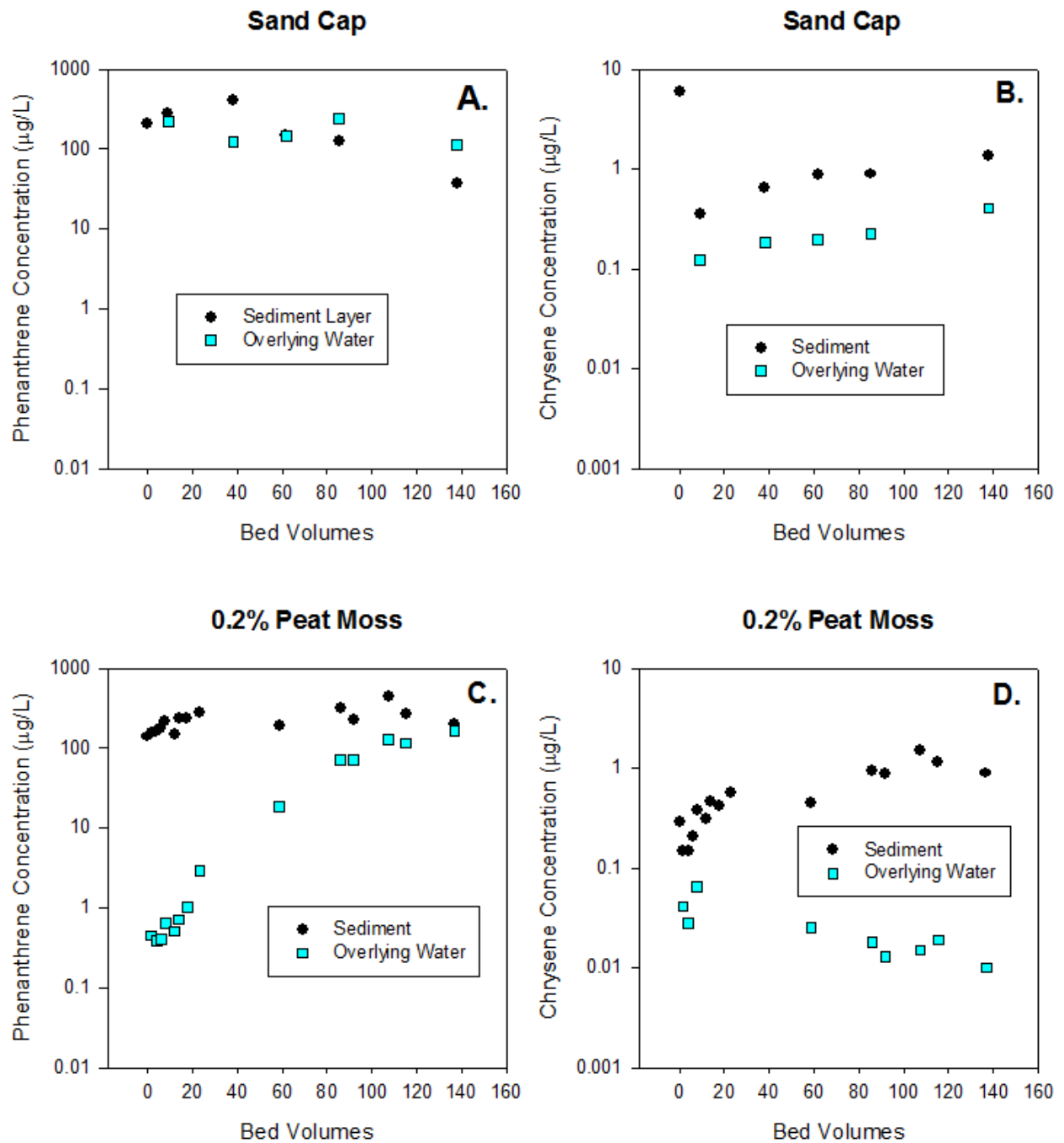


Figure 10. Phenanthrene and chrysene concentrations as a function of bed volumes in sediment caps without amendments and with peat moss amendment.

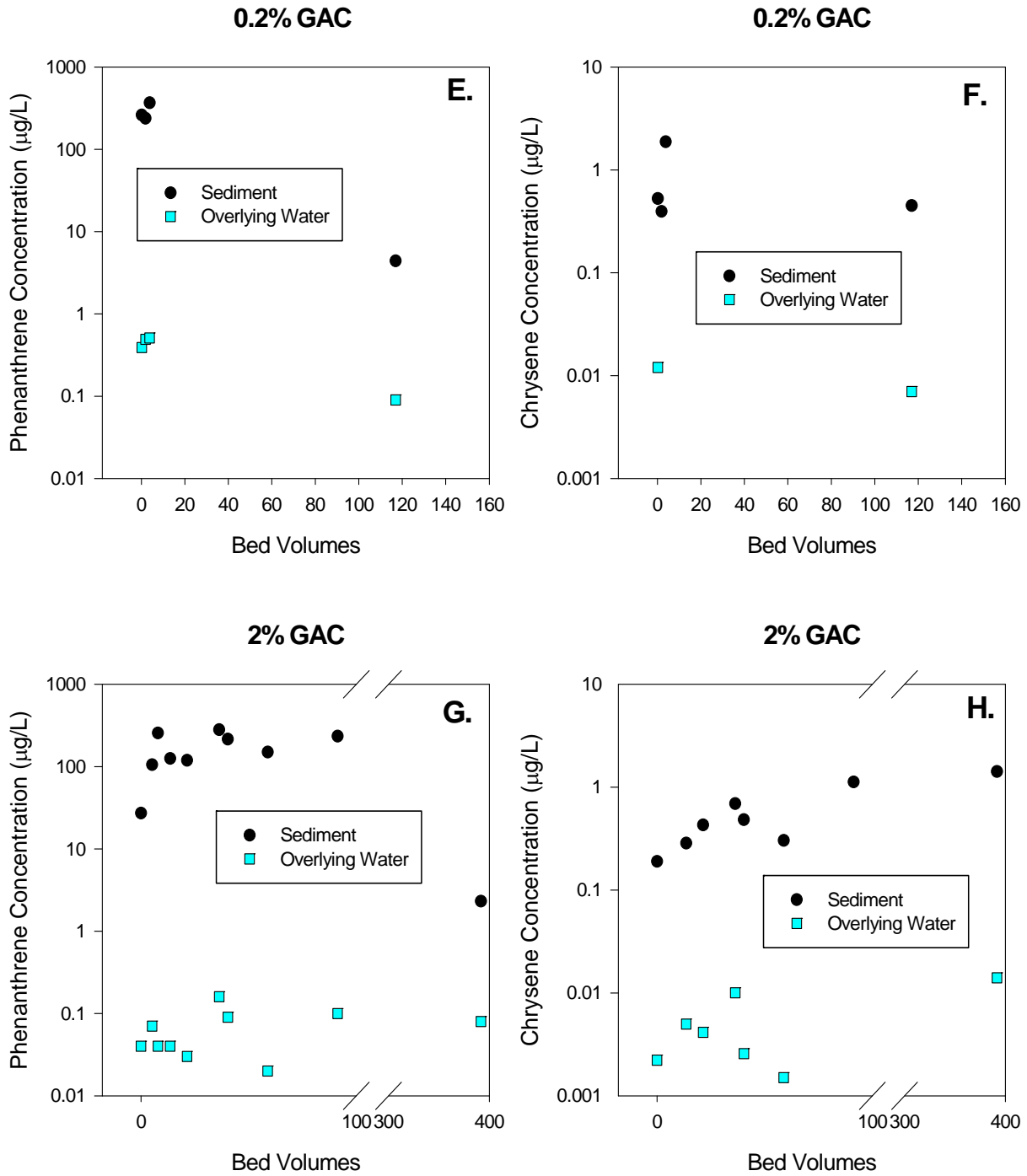


Figure 11. Phenanthrene and chrysene concentrations as a function of bed volumes in sediment caps with 0.2% and 2.0% activated carbon amendment.

v) Aqueous equilibrium experiments with sediment before and after flushing with water.

Sediment from the column studies were analyzed for PAH dissolution before and after exposure to flow in column experiments. These measurements were performed to evaluate how PAH dissolution changed as a function of exposure to water flushing in the column experiments. We expected to see a loss of the lower molecular weight PAHs from the sediment as a function of flushing. Sediment from two column experiments were taken after 4 months and 7 months of flow as described in results presented earlier for the unamended column experiments. The sediments were placed in batch vials with a solid to liquid ratio of 0.04 and allowed to equilibrate in the dark for 6 weeks. The water phase contained 1000mg/L NaN_3 as a biocide to minimize biological activity during the equilibrium experiment. Batch equilibrium experiments were also performed using sediment that had not been in a column, but was representative of the sediment initially placed in the columns. Low molecular weight PAHs were greatly reduced in both columns based on porewater measurements and batch experiments. Figure 12 shows the drastic reduction of acenaphthene (ACE) in batch experiments of the sediment placed in columns relative to sediment that had not been in a column. Other low molecular weight PAHs such as naphthalene and acenaphthylene appear to have depleted in the initial sediment.

In a column run for 4 months the acenaphthene concentration in the porewater collected at the end of the column experiment was 1.05 ug/L (not shown in a figure). When this sediment was placed in the batch experiment the acenaphthene concentration in the water phase doubled to 2.16 ug/L. This is possibly due to the greater contact between the sediment and the water phase in a batch experiment. In the column, many of the solid surfaces are touching other solid surfaces and not in contact with the water phase. In addition to this, there may be pore spaces which are not hydraulically connected to the flow of water through the column or the porewater sampling port. When the sediment is removed from the column and introduced in a batch slurry there is better contact between the water phase and contaminated sediment surfaces.

For a middle molecular weight PAH such as phenanthrene (PHN), a smaller decrease in equilibrium aqueous concentration is seen compared to acenaphthene. After 4 months in a column, aqueous equilibrium phenanthrene concentration is reduced by about half and is decreased further after 7 months in a column. Phenanthrene porewater concentration in the sediment collected from the column at the end of the 4 month experiment was at 37 ug/L (not shown in the figure) and only 18.4 ug/L from the batch experiment using the same sediment. It is possible that the creosote phase exposed to fluid flow in the columns may have developed an increased mole fraction of phenanthrene after 4 months. When this sediment is placed in a batch experiment, the fresh creosote surfaces that are now exposed do not

contribute additional phenanthrene to the porewater relative to the creosote surfaces that had already been exposed in the column and been enriched in phenanthrene.

For pyrene, there appears to be little change in aqueous concentration as a function of exposure to water flushing in the columns. This could be a result of the loss of pyrene mass being compensated by the faster loss of low molecular weight PAHs resulting in little change in the mole fraction of pyrene in the residual creosote phase. For a high molecular weight PAH, chrysene, (CHR) the concentrations in the batch water phase from the column material is higher than the sediment that was not placed in the column. This likely a result of the increased mole fraction of chrysene in the creosote phase of the sediment that was in the columns. Like phenanthrene, chrysene measurements from batch experiments after the column was run were smaller than porewater measurements at the end of the column. This can be explained for reasons similar to phenanthrene where the creosote trapped in immobile zones did not undergo change in mole fraction while the surfaces exposed to flow in the column were enriched with the higher molecular weight compounds.

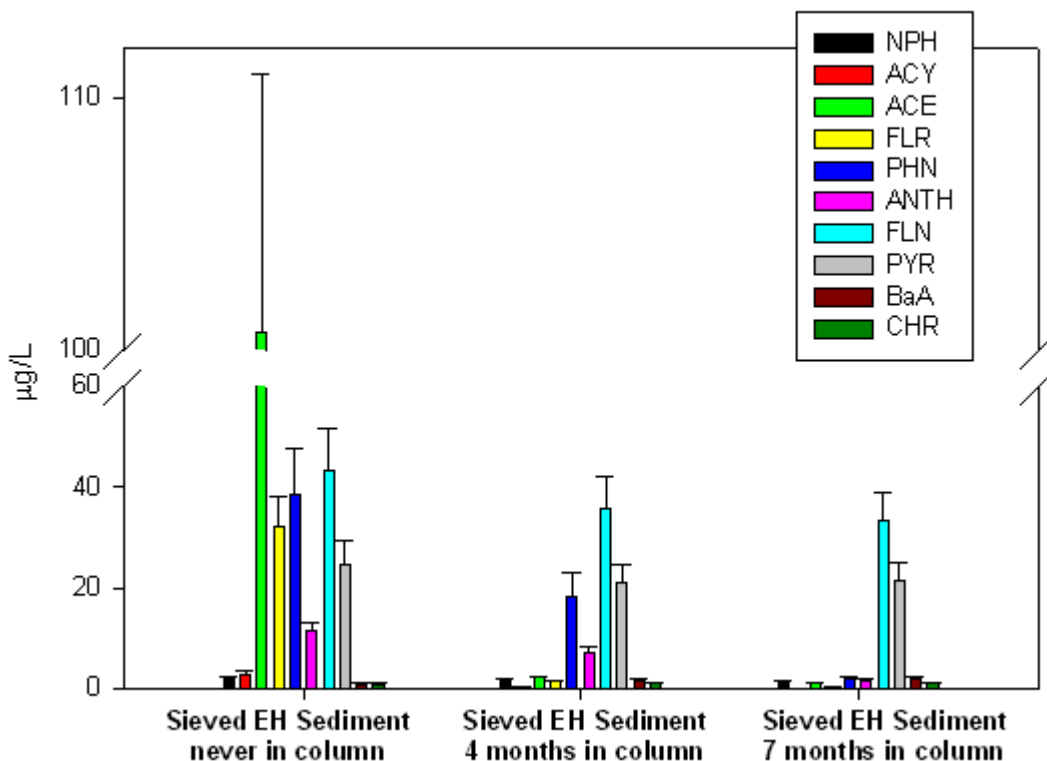


Figure 12. Eagle Harbor (EH) Sediment that was analyzed in batch equilibrium experiments (solid:liquid ratio 0.04) after it had been subjected to various stages of dissolution.

vi) PAH Migration in Biological Column Experiments

Azoic column experiments were performed to understand the effects of groundwater advection on PAH transport in Eagle Harbor capping material. A second scenario was desired to understand the effects of groundwater advection on PAH transport in biologically active systems. This is important because PAHs (once in the aqueous phase) can be significantly degraded (Wammer et. al. 2005, Bosma, T.N.P., et al. 1997). PAHs on the sediment-water surface have been suspected to degrade (Xia, X. et al. 2008). Bacteria attached to porous media can also increase the sorption capacity of the cap and degradation of those sorbed PAHs may also be possible (Hernan, D. C. et. al. 1997). Here, we sought to establish an optimal degradation experiment under aerobic conditions. In areas of groundwater upwelling, oxygen from the surface may be limited. However, anaerobic degradation may be possible with nitrate or sulfate serving as electron acceptors. Anaerobic degraders have been shown to degrade PAHs utilizing nitrate (McNally, D.L. et al. 1998), but the degradation rates are typically much slower compared to aerobic degradation.

First, a column was set-up and run without the addition of sodium azide. This column performed similar to systems with sodium azide (breakthrough of PAHs in the cap was rapid), and it was concluded that the column may not have been biologically active simply because the column was not killed with sodium azide. At this point, the sediment and capping material from Eagle Harbor had been stored at 4 degrees C for over a year. Both aerobic and anaerobic PAH degrading bacteria have been isolated from the Eagle Harbor site (Geiselbrecht, A.D. et al. 1998, Hedlund, B.P. et al. 2006, Tang, Y.J. et al. 2005). However, the native bacteria may have been inactive, or there may have been insufficient nutrients supplied by the sediment. In order to test for the presence of PAH degrading bacteria in Eagle Harbor sediment, batch experiments were conducted. Batch experiments were also conducted using freshly collected Anacostia River sediment. In addition, recent literature on sediment from the Anacostia River suggested that PAH degraders would be present and should be able to colonize a cap (Himmelheber, D.W. et al. 2008, Himmelheber, D.W. et. al. 2009).

The batch slurry experiments were started in 50 ml glass flasks containing 5 grams of sediment and about 40 ml of nutrient solution. The nutrient solution was selected based on work by previous researchers who used BOD nutrient buffer pillows (Knights et al. 2003), and nutrient mixtures from other researchers were considered (Wammer et al., 2005, Ripp et al. 2000). The flasks were capped with a foam plug to allow for aerobic conditions, but prevent the volatilization loss of low molecular weight PAHs. The flasks were placed on a shaker table and allowed to incubate while the contents were mixed up in a slurry. After two weeks, the sediment suspensions were considered ready to be used to seed batch culture experiments. Culture experiments were first repeated in 50 ml flasks and then repeated using

larger containers. Final culture batches were conducted in 4L flasks containing Teflon stir bars with large foam plugs. The batch cultures received a nutrient solution, a phenanthrene spike (2.25 ug) initially in methanol (15µL), and 5 drops of bacterial seed from the sediment slurries (both Eagle Harbor and Anacostia River). The small quantity of methanol present in spikes of 15 µL was not expected to impact micro-organisms or have an impact on biomass microbial activity (Knights, C.D. 2003). However, if bacteria were growing on methanol as a food source, the higher biomass could increase sorption of PAHs. Bacteria from the sediment slurry may have also contained a small amount of sediment. This would have had a larger effect on the smaller 50ml batch experiments than the larger 500ml or 4L ones. Figure 13 shows the results of phenanthrene measurements in the aqueous phase of the 50 ml batch experiments using SPME with alum flocculation.

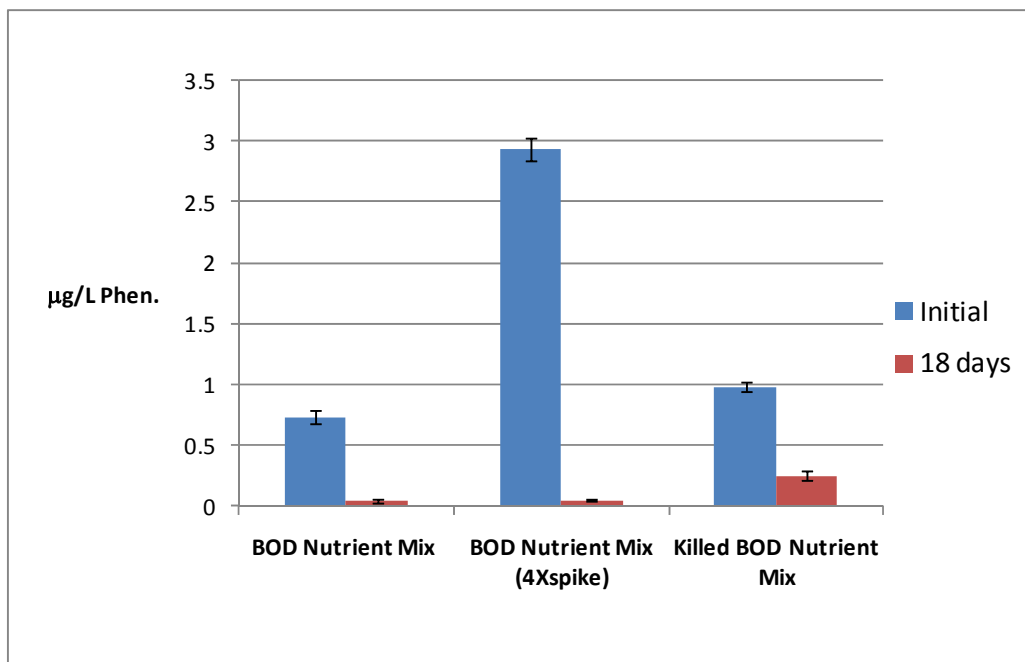


Figure 13. Phenanthrene depletion in 50 ml Batch Culture Experiments.

It can be seen that after 18 days, phenanthrene loss was observed in all batch experiments. It appears that the greatest removal occurred in experiments with no sodium azide added. Error bars represent one standard deviation and are based on 2 to 4 replicates. It was suspected that initial losses of phenanthrene in the BOD nutrient mix over the killed (500mg/L NaN₃) BOD nutrient mix was due to fast

degradation (in the BOD nutrient mix) or sorption of PAHs to biomass. The killed BOD nutrient mix may have showed a depletion of phenanthrene due to sorption to sediment in the bacteria seed or sorption onto dead biomass. In order to minimize sorption of PAHs onto organics introduced with the bacterial seed, larger batch culture experiments were performed. These second set of experiments were performed in larger 500ml jars with Teflon stir bars to maintain well mixed conditions. These larger experiments were again capped with a foam plug and were sampled initially, and at 4 and 10 days (Figure 14).

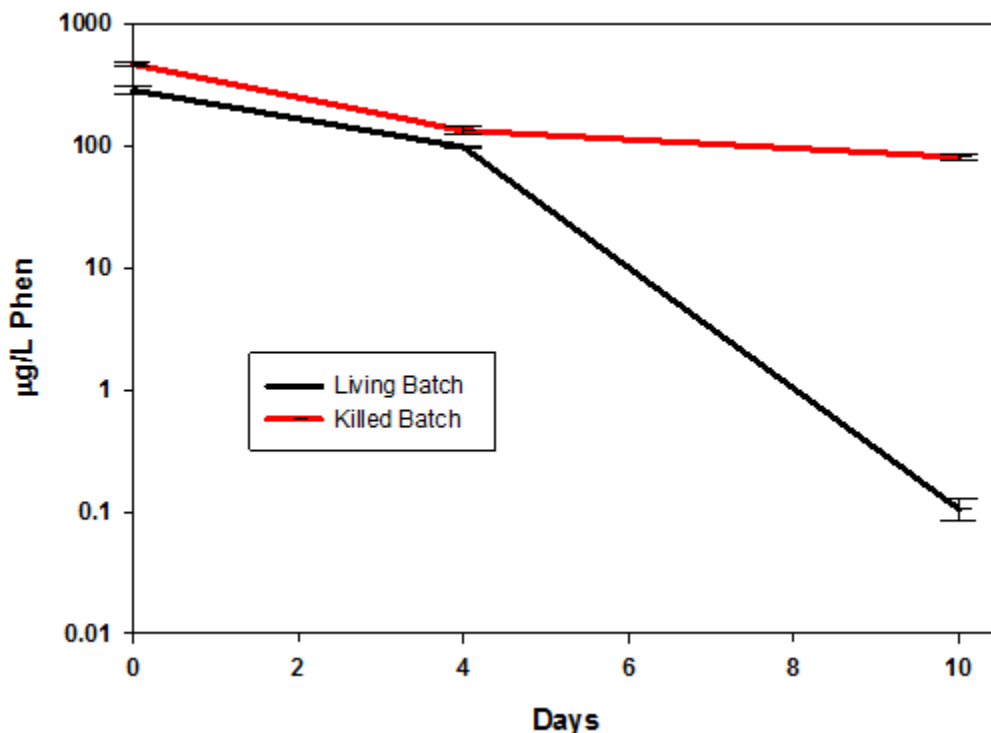


Figure 14. Phenanthrene depletion over time in biologically active and inactive batch experiments.

The experiment shown in Figure 14 shows that phenanthrene could be depleted to levels several orders of magnitude smaller than starting concentrations when the batch system was not killed with sodium azide. Both the “living” and killed experiment were spiked with the same amount of phenanthrene (8000 ug) dissolved in methanol (40uL) and spiked with 2ml of bacterial seed. The only difference was the presence of sodium azide or small variations in the suspended solid content or biomass content of the bacterial seed. Again, losses were seen in both batch experiments. In the batch killed with sodium azide, the rate of loss was much greater during the first four days compared to the latter period.

It was suspected that we might be observing the sorption of PAHs onto bacteria growing on methanol. To check for this possibility, phenanthrene dissolved in methanol was spiked into an empty glass

jar and the methanol was allowed to evaporate overnight. The glass jars were then filled with water and the phenanthrene was allowed to dissolve into the water phase and a solution of 178 $\mu\text{g/L}$ phenanthrene was produced within a few days. This solution was used in three batch experiments. First, a batch experiment with nutrients and a bacterial seed. Second, a batch with nutrients and no bacterial seed. Third, a killed batch with nutrients and a bacterial seed. In the first batch, the phenanthrene concentration depleted to 1.3 $\mu\text{g/L}$ after 4 days. In the second batch, with no bacterial seed, the concentration decreased to 72 $\mu\text{g/L}$, and the killed batch concentration showed a measured increase to 262 $\mu\text{g/L}$ after 4 days. Calibration checks showed that the SPME calibration was valid. It is uncertain what caused the concentration changes in this final experiment.

With the confirmation of PAH degrading bacteria in the culture solutions, the first biologically active column experiment was started. A 4 L batch culture was created and allowed to deplete the phenanthrene concentration down to 1.9 $\mu\text{g/L}$. At this point, the absorbance of the solution was measured at 660NM to be 0.016, which is the wavelength often used for estimating biomass concentration via optical density (Koch, A.L., 1994).

Column experiments were constructed using capping material that had been inoculated with the PAH degrading bacterial culture. The configuration of this biological column was slightly altered from that of the earlier azoic columns. A thin layer of glass beads was placed between the sediment and the capping layer in the biological column. An effort was made to place port 1 at this layer of glass beads to get a more accurate measure of the PAH inputs to the cap. However, due to some settlement of either the glass wool below the sediment, or the sediment itself, port 1 ended up being located 1 cm into the capping material. This can be seen in Figure 15 on the column depicted on the y-axis. It can also be seen that the distance of the overlying water (OW) was shortened (to 9.5 cm) and sampling of this layer was not done through a port, but rather, using a glass Pasteur pipet from the top of an open column. Column effluent was allowed to overflow out of port 6. The length of the capping material remained the same (65 cm) and the sediment layer was shortened (to 10 cm). The biological column was operated for 71 days with the last sampling taken at 48 days (91.7 bed volumes). Porewater concentrations have been measured for 12 PAH compounds from 5 ports along the cap and the overlying water. In addition to the small structural changes, it is likely that the source zone is different compared to earlier azoic columns. This makes it a little difficult to make direct comparisons between the azoic and this biologically active column. However, if we take port 1 concentrations to be a source input to the rest of the cap, it is possible model the system using CXTFIT code. Figure 15 focuses on the migration of phenanthrene through the biological cap for various bed volumes (listed in the legend). At low bed volumes (initially) phenanthrene concentrations are high at port 1 (inlet) and progressively decreases up through the column. However,

after only 2 bed volumes (green diamonds in Figure 15), phenanthrene appears halfway through the cap. At longer times, the source of phenanthrene in sediment appears to have depleted and the higher concentrations are seen near the top of the cap as the PAHs are flushed out of the cap. Thus, there appears to be little improvement of PAH breakthrough in a biologically active sand cap over an azoic sand cap. Overlying water concentrations are indicated by corresponding solid lines at the top of the figure.

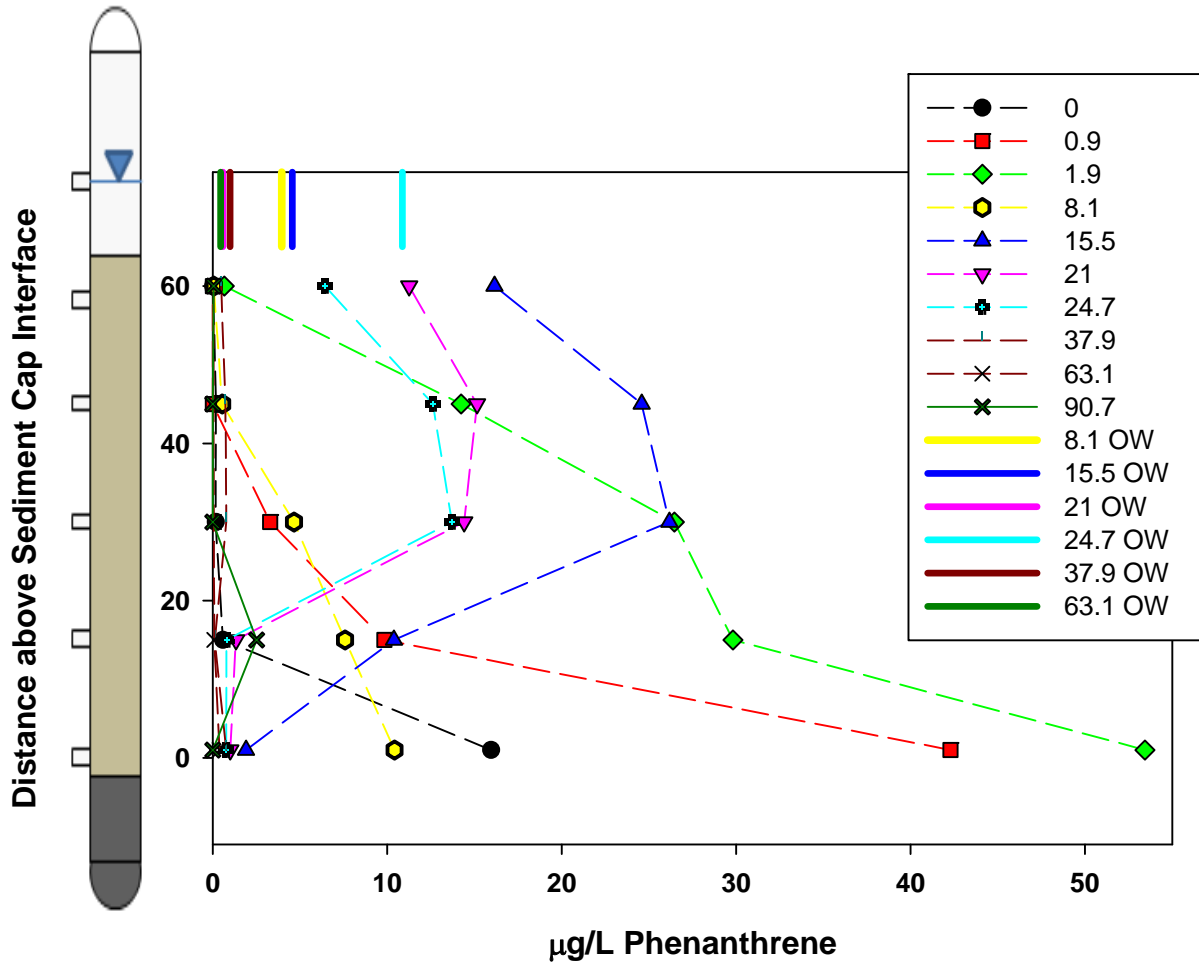


Figure 15. Migration of Phenanthrene through the biologically active capping material at different bed volumes (indicated by the numbers in the legend)

vii) Modeling PAH migration in sediment caps

The mathematical model for PAH dissolution from the creosote phase was used to predict the change in PAH concentrations in the creosote phase and water phase as illustrated in Figures 16 and 17. However, aqueous concentrations of low molecular weight PAHs in our model don't drop off as rapidly as in the model produced by Peters et al. (1999) which is likely due to differences in the implementation of the mass transfer rate constants. Additionally, when conducting model verification, the mass balance for two PAHs (anthracene and chrysene) do not close. These are the two PAHs that were expected to form a solid precipitate (Peters, C. et al., 1999).

As seen in Figure 16, the concentration of naphthalene is depleted rapidly in the first few years of flushing at typical groundwater velocities. However, the higher molecular weight compounds such as chrysene is seen to increase in concentration with time due to the much faster loss of the low molecular weight compounds. This phenomena is manifested in the aqueous concentration as well in Figure 17, where, the lower molecular weight compounds are seen to decrease with time and the higher molecular weight compounds are seen to increase with time.

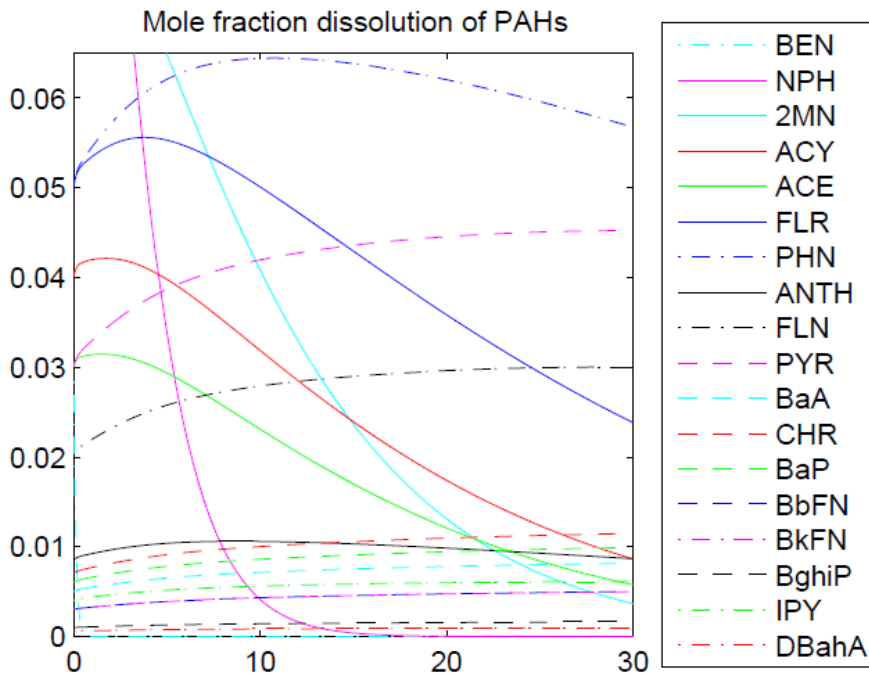


Figure 16. Mole fractions of PAHs in the creosote phase over 30 years.

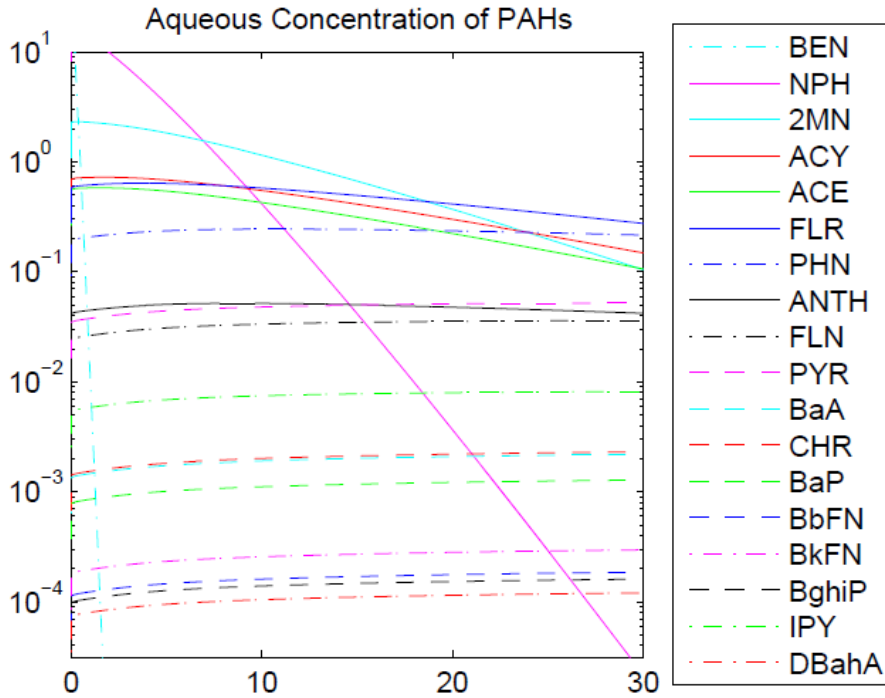


Figure 17. Aqueous PAH concentrations in the pore water over 30 years

The observed migration of PAHs through the capping material was modeled using an analytical solution to the one dimensional advection-dispersion equation with retardation (Ogata and Banks, 1961). Pyrene was chosen to be used in the analytical model because its concentration in the sediment layer remained relatively constant for the duration of the experiment, and a constant boundary condition was a reasonable assumption. A constant influent pyrene concentration in the porewater from the sediment layer (C_0) was assumed to be the average of the observed sediment porewater concentration for the analytical model. A tracer test shown in Figure 18 was used to obtain a pore velocity of 121 cm/day (126.5 cm/day for 0.2% TOC amended column) and an effective porosity of 0.25 (0.24 for TOC amended column). Chloride was assumed to be a conservative tracer for columns with and without amendments. Others have found that chloride can be retarded by cytoplasm (closed pores) in pure peat systems (Price et al., 2009). The assumption is being made that the small peat moss contents mixed in these columns does not impact chloride retention. A column length of 60 cm was used for the tracer studies (cap only) and was used for calculations. The linear hydrodynamic dispersion coefficient (D) was 225 cm²/day (155 cm²/day for TOC amended cap). The capping material bulk density (ρ_b) was taken to be 1.7 kg/L for columns with and without amendments. The retardation factors (R) for no amendment, 0.2% TOC and

0.2 % GAC were 28, 101 and 7×10^7 respectively. Hydrodynamic conditions for GAC amended caps were assumed to be the same as non-amended caps.

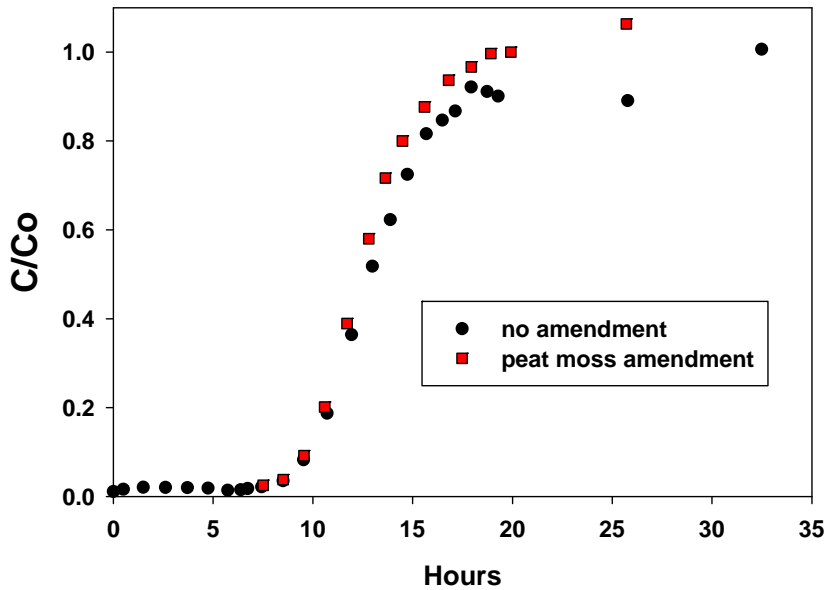


Figure 18. Tracer study results of laboratory column experiment showing transition from DI water to CaCl_2 solution for capping material with no amendment and peat moss amendment.

Figure 19 shows the spatial migration of pyrene in the columns compared to several model simulations. Experimental pyrene migration exceeds model predictions in both amended and non-amended caps when looking at the cap near the column outlet. Deviations between the experimental results and a model can be attributed to four factors: First, column construction advances the pyrene migration initially which is not captured by the model. Second, the influent pyrene concentration (sediment pore water from port 1) was not constant, but increased over the time range being modeled. The average sediment pyrene porewater concentration for each particular column (amended or non-amended) was used as a constant input in the Ogata-Banks analytical solution (generally all concentrations were within $\pm 5 \mu\text{g/L}$ of the calculated average pyrene concentration). This model assumes a constant input of PAHs for all times (this is more problematic when measuring some of the other PAHs which had more source concentration changes due to dissolution processes). The experimental measurements of pyrene in the sediment layer was used as a fluctuating input to the advection-dispersion equations solved by CXTFIT software (Toride, N. et al. 1999) to model pyrene migration in the column capping material when equilibrium partitioning is the primary mechanism for retardation in the cap. The CXTFIT code using a constant input matched the Ogata and Banks solution closely (Figure 19). Third,

PAHs and other organic compounds present in the sediment porewater could compete for sorption, effectively reducing the apparent K_d values (as seen in batch experiments for pyrene). Fouling from other organics present (e.g. humic acids) in sediment has been observed to reduce the effectiveness of PAH sorption in chars (Pignatello, J.J., et al., 2006). Fourth, the equilibrium partitioning assumption inherent in the calculation of the retardation factor may not be accurate due to the short fluid residence time in the column and possible existence of immobile zones within the column. This could be the case given a porosity of 0.47 (greater than 0.24 or 0.25 from tracer test) calculated from the specific gravity of the cap, bulk density of the cap, and the specific weight of water. The modeling utilized porosity measurements from the tracer studies. However, sorption sites trapped in immobile zones may have reduced the % TOC available to an effectively smaller TOC content.

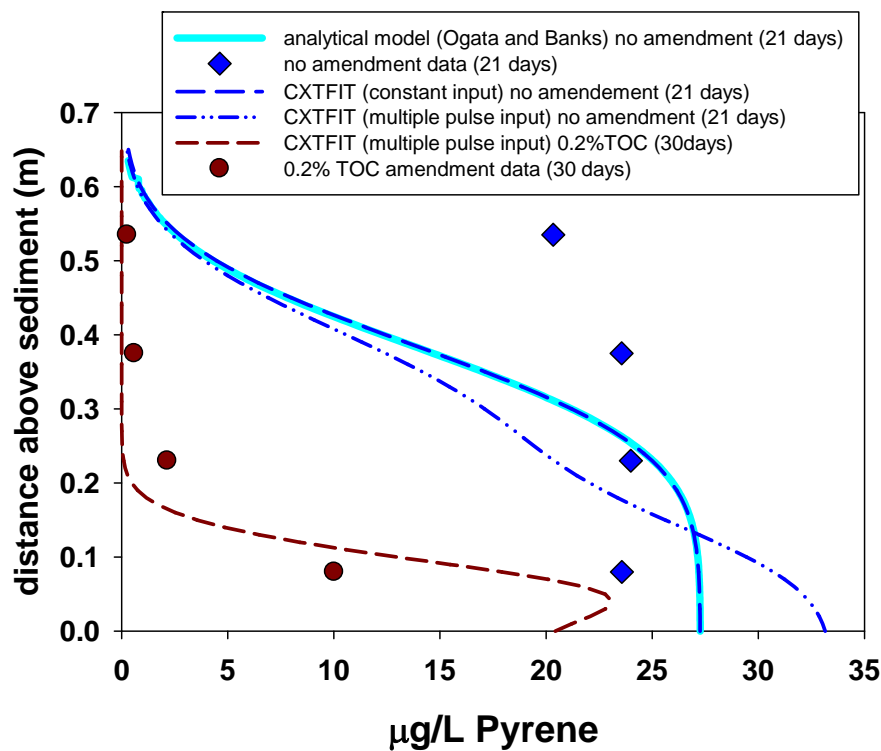


Figure 19. Spatial Migration of Pyrene in Columns not amended and amended with 0.2% TOC with comparisons between analytical and CXTFIT models.

The observed migration of phenanthrene through the capping material was modeled using the CXTFIT code. Figure 20 shows the temporal migration of phenanthrene in the columns compared to several model simulations. Experimental phenanthrene migration compared well with model predictions when contrasting the various capping treatments. The experimental measurements of phenanthrene in the sediment layer (port 1) was used as a fluctuating input to the advection-dispersion equations solved by CXTFIT software (Toride, N. et al. 1999) to model phenanthrene migration in the column capping material when equilibrium partitioning is the primary mechanism for retardation in the cap. Deviations between the experimental results and a model are attributed to three factors: First, due to the limited number of SPME collection points some of the concentration changes in the source zone may have been missed. Second, PAHs and other organic compounds present in the sediment porewater could compete for sorption, effectively reducing the apparent K_d values. Fouling from other organics present (e.g. humic acids) in sediment has been observed to reduce the effectiveness of PAH sorption in chars (Pignatello, J.J., et al., 2006). Third, the equilibrium partitioning assumption inherent in the calculation of the retardation factor may not be accurate due to the short fluid residence time in the column and possible existence of immobile zones within the column.

The predicted concentration of PAHs in the GAC amended column was near zero and the measured aqueous concentrations were also close to or below the quantitation limits. As described earlier, none of the PAHs were seen to break through the GAC amended columns and this is what the model also predicted.

Modeling of biological systems showed that no noticeable degradation should be expected in the porewater of the columns during the short residence times operated in the experimental column. However, if a biofilm develops in the cap solids, biodegradation rates can compete with the rate of flushing. What is also likely to occur is an increased sorption of PAH to attached growth on the capping material in a biologically amended system. This is most likely the cause of the reduced phenanthrene concentrations in the biologically amended column compared to the model shown in Figure 20.

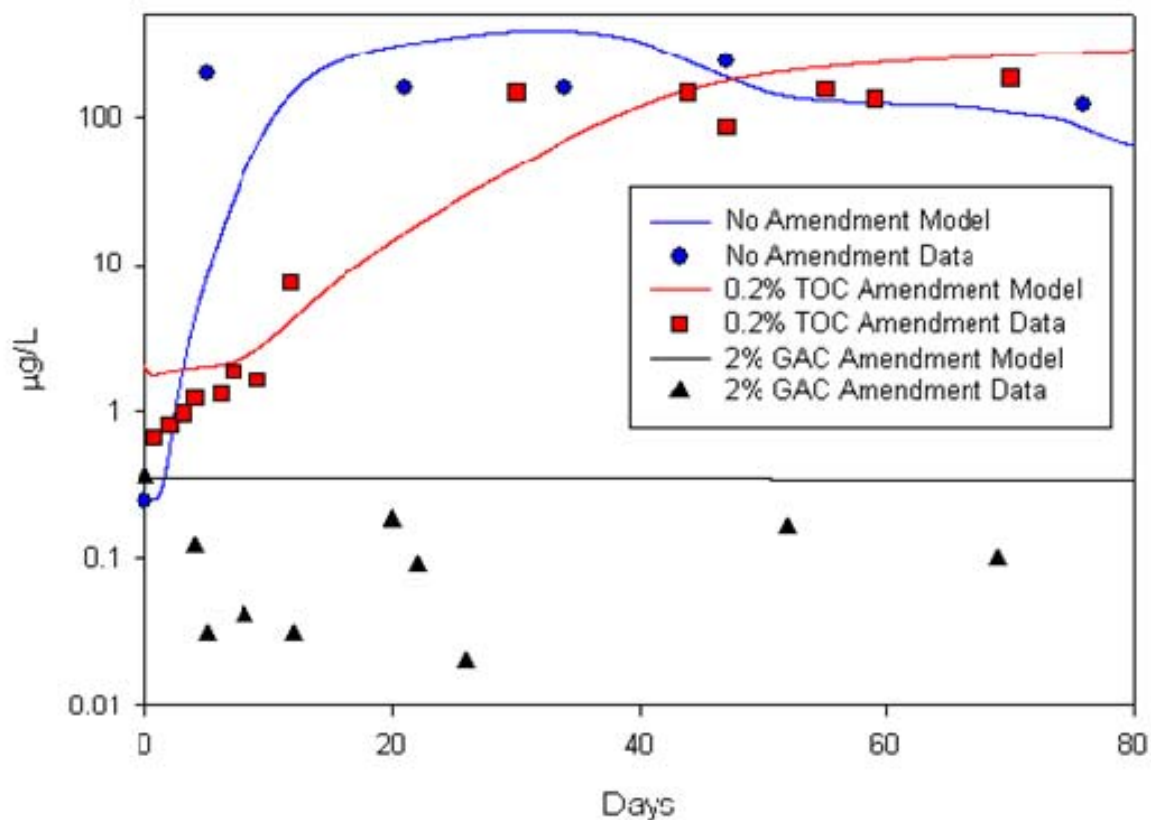


Figure 20. Phenanthrene migration at Port 5 over time in non-amended, peat amended, and GAC amended columns and model predictions. The GAC data are below the limit of quantification for SPME.

The impact of biodegradation on overall contaminant transport through a porous media is strongly influenced by the relative rates of degradation and advection. At high Darcy velocity, residence time is too short to observe a concentration decrease due to biodegradation. The column studies performed in the laboratory were operated at a Darcy velocity of 0.015 m/hr due to limitations with maintaining low flowrates through a column and also challenges with the length of time required to observe close to breakthrough when flowrates are small. The transport model with parameters derived from laboratory experimental observations was used to perform simulations of biodegradation in the column operating at different Darcy velocities. As shown in Figure 21, breakthrough starts close to 20 bed volumes at a Darcy velocity of 0.015 m/hr and there is little difference between a biologically active and inactive column at this flow rate. The residence time is too short for biodegradation to have an

impact. When the Darcy velocity is reduced 100-fold to 0.00015 m/hr, the effect of biodegradation is more apparent. Thus, biodegradation will play a role in PAH retention within the cap when groundwater velocities are small and biodegradation rates are favorable compared to the flushing rate. Also, it is important to remember that the biodegradation modeling is limited to degradation by organisms present in the water phase. If an actively degrading biofilm develops on the cap solids over time, the effective biodegradation rates could be enhanced. However, this was not observed in the duration of laboratory column experiments.

Extending the model parameterized using experimental measurements we can simulate long-term performance of the columns. Shown in Figure 22 is a simulation of phenanthrene breakthrough in columns amended with peat moss (TOC of 0.2%, 0.5%, and 2%) and activated carbon (GAC of 0.002% and 0.2%). The input concentration to the cap is assumed to be constant at 100 $\mu\text{g/K}$ of dissolved phenanthrene. As illustrated in Figure 22, peat moss (a surrogate for natural organic matter) is much less effective in retarding phenanthrene compared to activated carbon. At 0.2% TOC in the form of peat moss in the cap, phenanthrene breakthrough takes place in a couple of months and with a higher dose of peat moss at 2% TOC, the breakthrough is delayed to 8 months. A very small dose of GAC (0.002%) breakthrough is delayed to 10 years and with 0.2% AC, the breakthrough is longer than 1000 years. These simulation results explain why the laboratory experiments with 0.2 and 2% GAC in the cap did not observe PAH breakthrough over 6 months of monitoring. It is possible that mass transfer limitations within carbon particles and fouling of the carbon with other organic molecules may degrade long-term performance to some extent. However, with the large reductions in PAH transport evident from the laboratory experiments and modeling simulations with GAC amended sand caps, it appears promising to include GAC amendments in sand caps to enhance performance where groundwater advection is of concern.

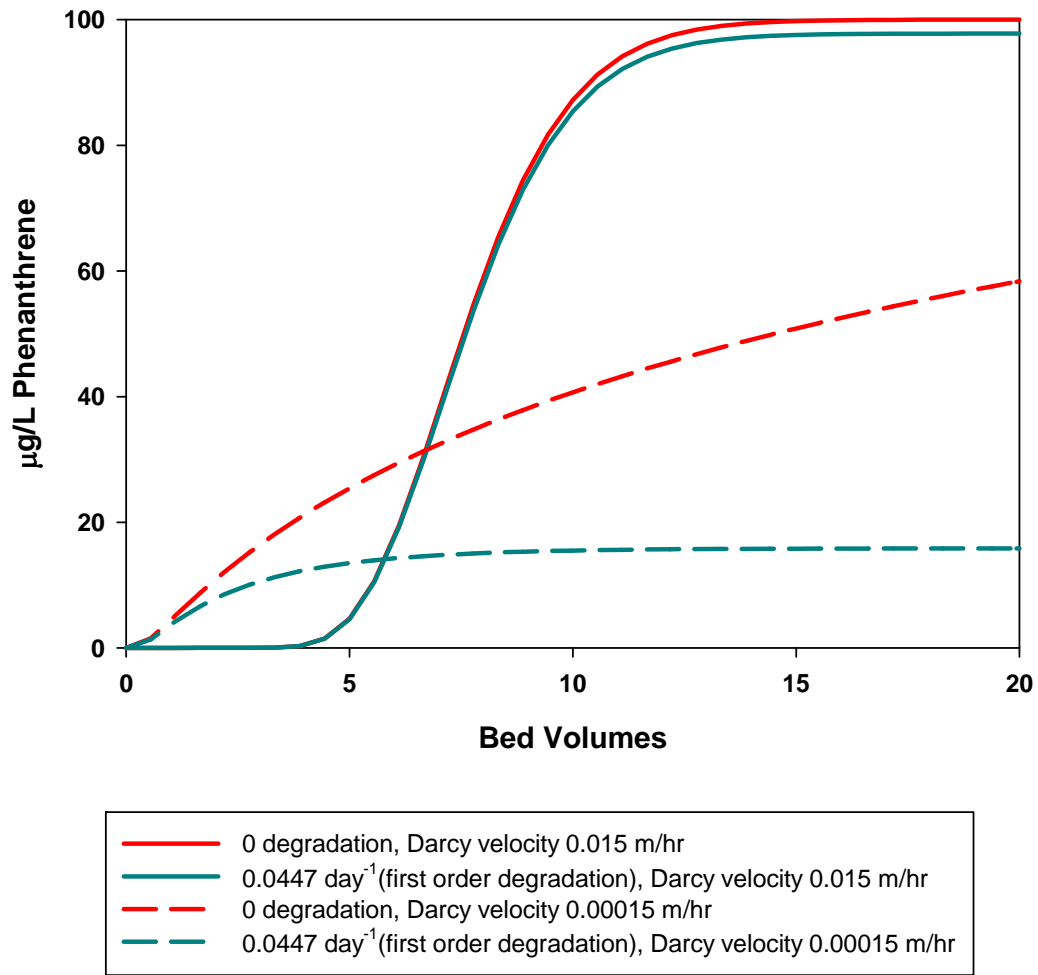


Figure 21. Effect of Darcy velocity on biodegradation in cap

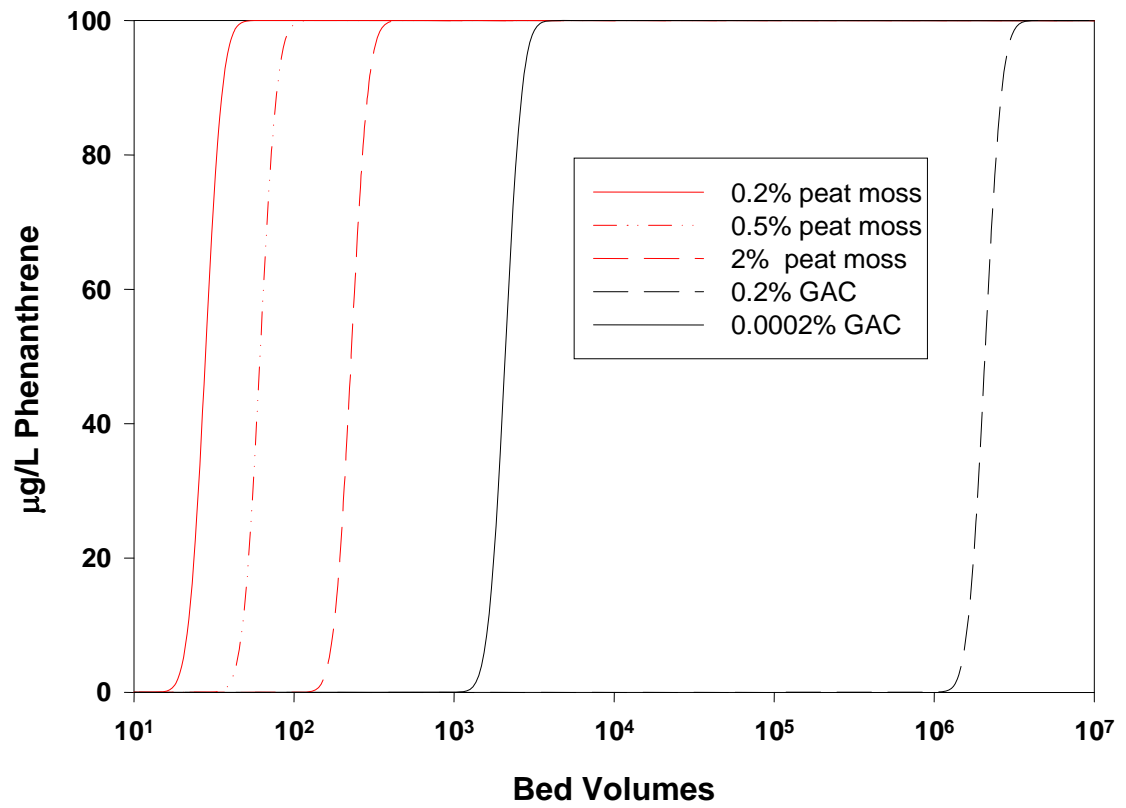


Figure 22. Effect of peat moss and GAC amendment on breakthrough times of phenanthrene in sand cap.

VI. CONCLUSIONS AND RECOMMENDATIONS

The main conclusions of this study are as follows:

- 1) PAH dissolution of a creosote contaminated sediment can be described by Raoult's law
- 2) There is potential of PAH breakthrough in typical low organic carbon sand caps placed in the field when there is groundwater advection.
- 3) Amendment of sediment caps with natural organic matter in the form of peat moss is moderately successful in reducing PAH transport.
- 4) Amendment of sediment caps with activated carbon in the range of 0.2 – 2% by weight greatly reduces PAH transport through a sand cap.
- 5) The dissolution and transport of PAHs in a sand cap can be modeled in two phases: the first phase describing the time variant dissolution process from creosote and the second phase involving retarded transport through the capping material.
- 6) Measurement of PAH concentration in cores taken out of sediment caps is a poor indicator of contaminant breakthrough, especially in cases where there is little capacity in the cap material to bind contaminants.
- 7) Experiments with sediment caps with and without biological activity did not show remarkable difference for the flow conditions tested. It is possible that in the long-term over many years, a biological community in the form of biofilms may develop in the capping material that adds to the effectiveness of the cap in limiting contaminant migration.

The main recommendations for future work based on this study are:

- 1) The next step in the technology transition process should involve pilot-scale testing of amended sand caps placed over contaminated sediments at a site where groundwater flow has been documented. A long-term monitoring plan should evaluate migration of porewater contaminants through the cap over time for variously amended caps.
- 2) Additional laboratory-scale research is needed to develop efficient methods to deploy amendments to caps without having the sand and amendment segregate during placement under water due to density differences. Delivery of amendments through specially manufactured pellets such as SediMite™ (ESTCP project ER-0835) could be a viable option but needs to be tested. The sorbents could be delivered to achieve an uniform distribution within the cap or as a distinct layer within the cap. Engineering feasibility and effectiveness of either approach needs to be tested in the field.

VII. LIST OF PUBLICATIONS

List of Papers

Paper 1: SPME Measurement of Porewater PAH Transport in Amended Sediment Caps

Philip Gidley, Seokjoon Kwon, and Upal Ghosh (in preparation)

List of Posters/Presentations

1. Characterization of Contaminant Transport Through In-Place Sediment Caps-Poster

P. Gidley, L. Lockard, S. Kwon, U. Ghosh

29th Annual Graduate Research Conference

University of Maryland Baltimore County, Baltimore, MD 4-24-07

2. Characterization of Contaminant Transport Through In-Place Sediment Caps-Poster

P. Gidley, L. Lockard, S. Kwon, U. Ghosh

Society of Environmental Toxicology and Chemistry (SETAC), Chesapeake and Potomac Regional Chapter Meeting

Laurel, MD 4-07

3. Measurement of Porewater PAH Transport in Sediment Caps using Solid-phase Microextraction(SPME)-Presentation

P. Gidley, S. Kwon, U. Ghosh

Connecting people-Linking the fundamental concepts of sediment pollution remediation and ecotoxicity for improved engineering designs

Newcastle University, Newcastle, England 11-2-07

4. SPME measurement of porewater PAH transport in amended sediment caps-Presentation

P. Gidley, S. Kwon, U. Ghosh

SETAC North America 28th Annual Meeting

Milwaukee, WI 11-18-07

5. Characterization of Contaminant Transport through In-Place Sediment Caps-Poster

P. Gidley, S. Kwon, U. Ghosh

Gordon Research Conference, Environmental Sciences: Water

Holderness, NH 6-25-08

6. SPME measurement of porewater PAH transport in amended sediment caps-Presentation

P. Gidley, S. Kwon, U. Ghosh

SETAC North America 29th Annual Meeting

Tampa, FL 11-18-08

7. Porewater PAH transport in amended sediment caps-Poster

P. Gidley, S. Kwon, U. Ghosh

American Geophysical Union (AGU) meeting

Toronto, ON 5-22-09

8. Modeling and SPME measurement of porewater PAH transport in amended sediment caps-Poster

P. Gidley, N. Agarwal, S. Kwon, and U. Ghosh

Strategic Environmental Research and Development Program (SERDP), Partners in Environmental Technology Technical Symposium & Workshop

Washington, D. C. 12-2-09

VII. REFERENCES

- Azcue J.M.; Zeman, A.J.; Mudroch, A.; Rosa, F.; Patterson, T.. Assessment of sediment and porewater after one year of subaqueous capping of contaminated sediments in Hamilton Harbor, Canada. *Water Science & Technology*. Vol. 37, no. 6-7, pp. 323-329. 1998.
- Ball, W.P., (1991) Long-Term Sorption of Halogenated Organic Chemicals by Aquifer Material. 1. Equilibrium. *Environ. Sci. Technol.* Vol. 25, No7. 1223-1237
- Barth, E. F., D. Reible, et al. (2008). "Evaluation of the Physical Stability, Groundwater Seepage Control, and Faunal Changes Associated with an AquaBlok[®] Sediment Cap." *Remediation* **18**(4): 63-70.
- Boehm, A. B., G. G. Shellenbarger, et al. (2004). "Groundwater Discharge: Potential Association with Fecal Indicator Bacteria in the Surf Zone." *Environmental Science and Technology* **38**(13): 3558-3566.
- Bosma, T. N. P., P. J. M. Middelorp, et al. (1997). "Mass Transfer Limitation of Biotransformation: Quantifying Bioavailability." *Environmental Science and Technology* **31**(1): 248-252.
- Brenner, R. C., V. S. Magar, et al. (2002). "Characterization and FATE of PAH-Contaminated Sediments at the Wyckoff/Eagle Harbor Superfund Site." *Environmental Science and Technology* **36**(12): 2605-2613.
- Brenner, R. C., V. S. Magar, et al. (2004). "Long-Term Recovery of PCB-Contaminated Surface Sediments at the Sangamo-Weston/Twelve Mile Creek/Lake Hartwell Superfund Site." *Environmental Science and Technology* **38**(8): 2328-2337.
- Burnett, W. C., H. Bokuniewicz, et al. (2003). "Groundwater and pore water inputs to the coastal zone." *Biogeochemistry* **66**: 3-33.
- Coates, J. D., R. T. Anderson, et al. (1996). "Anaerobic Hydrocarbon Degradation in Petroleum-Contaminated Harbor Sediments under Sulfate-Reducing and Artificially Imposed Iron-Reducing Conditions." *Environmental Science and Technology* **30**(9): 2784-2789.
- Cornelissen, G., O. Gustafsson, et al. (2005). "Extensive Sorption of Organic Compounds to Black Carbon, Coal, and Kerogen in Sediments and Soils: Mechanisms and Consequences for Distribution, Bioaccumulation, and Biodegradation." *Environmental Science and Technology* **39**(18): 6881-6895.
- Cornelissen, G., G. D. Breedveld, et al. (2006). "Strong Sorption of Native PAHs to Pyrogenic and Unburned Carbonaceous Geosorbents in Sediments." *Environmental Science and Technology* **40**(4): 1197-1203.
- Cornelissen, G. and O. Gustafsson (2004). "Sorption of Phenanthrene to Environmental Black Carbon in Sediment with and without Organic Matter and Native Sorbates." *Environmental Science and Technology* **38**(1): 148-155.
- Deane, G., Z. Chroner, et al. (1999). "Diffusion and Sorption of Hexachlorobenzene in Sediments and Saturated Soils." *Journal of Environmental Engineering* **125**(8): 689-696.
- Deepthi, H. U., T. Tecon, et al. (2009). "Unlike PAHs from Exxon Valdez Crude Oil, PAHs from Gulf of Alaska Coals are not Readily Bioavailable." *Environmental Science and Technology* **43**(15): 5864-5870
- Ecosystem-Based Rehabilitation Plan - An Integrated Plan for Habitat Enhancement and Expedited Exposure Reduction in the Lower Fox River and Green Bay, *Independent Expert Panel report submitted to Wisconsin DNR*. December 20, 2001.
- Eek, E., G. Cornelissen, et al. (2008). "Diffusion of PAH and PCB from contaminated sediments with and without mineral capping; measurements and modelling." *Chemosphere* **71**: 1629-1638.

- Eek, E., O. Godoy, et al. (2007). "Experimental determination of efficiency of capping materials during consolidation of metal-contaminated dredged material." Chemosphere **69**: 719-728.
- Ghosh, U., A. S. Weber, et al. (1999). "Granular Activated Carbon and Biological Activated Carbon Treatment of Dissolved and Sorbed Polychlorinated Biphenyls." Water Environment Research **71**(2): 232-240.
- Go, J., D. J. Lampert, et al. (2009). "Predicting contaminant fate and transport in sediment caps: Mathematical modelling approaches." Applied Geochemistry **24**: 1347-1353.
- Guerin, W. F. and G. E. Jones (1989). "Estuarine Ecology of Phenanthrene-Degrading Bacteria." Estuarine, Coastal and Shelf Science **29**: 115-130
- Hatheway, A. W. (2002). "Geoenvironmental protocol for site and waste characterization of former manufactured gas plants; worldwide remediation challenge in semi-volatile organic wastes." Engineering Geology **64**: 317-338.
- Hawthorne, S. B., C. B. Grabanski, et al. (2006). "Measured Partitioning Coefficients for Parent and Alkylated Polycyclic Aromatic Hydrocarbons in 114 Historically Contaminated Sediments: Part 1. K_{oc} Values." Environmental Toxicology and Chemistry **25**(11): 2901-2911.
- Hawthorne, S. B., C. B. Grabanski, et al. (2005). "Solid-Phase Microextraction Measurement of Parent and Alkyl Polycyclic Aromatic Hydrocarbons in Milliliter Sediment Pore Water Samples and Determination of K_{DOC} Values." Environmental Science and Technology **39**(8): 2795-2803.
- Hernan, D. C., R. J. Lenhard, et al. (1997). "Formation and Removal of Hydrocarbon Residual in Porous Media: Effects of Attached Bacteria and Biosurfactants." Environmental Science and Technology **31**(5): 1290-1294.
- Herrenkohl, M. J., J. D. Lunz, et al. (2001). "Environmental Impacts of PAH and Oil Release as a NAPL or as Contaminated Pore Water from the Construction of a 90 cm In Situ Isolation Cap." Environmental Science and Technology **35**(24): 4927-4932.
- Himmelheber, D. W., K. D. Pennell, et al. (2007). "Natural Attenuation Processes during In Situ Capping." Environmental Science and Technology **41**(15): 5306-5313.
- Himmelheber, D. W., M. Taillefert, et al. (2008). "Spatial and Temporal Evolution of Biogeochemical Processes Following In Situ Capping of Contaminated Sediments." Environmental Science and Technology **42**(11): 4113-4120.
- Himmelheber, D. W., S. H. Thomas, et al. (2009). "Microbial Colonization of an In Situ Sediment Cap and Correlation to Stratified Redox Zones." Environmental Science and Technology **43**(1): 66-74.
- Hong, L., U. Ghosh, et al. (2003). "PAH Sorption Mechanisms and Partitioning Behavior in Lampblack-Impacted Soils from Former Oil-Gas Plant Sites." Environmental Science and Technology **37**(16): 3625-3634.
- Hyun, S., C. T. Jafvert, et al. (2006). "Laboratory studies to characterize the efficacy of sand capping a coal tar-contaminated sediment." Chemosphere **63**.
- Imhoff, P. T., P. R. Jaffe, et al. (1993). "An experimental study of complete dissolution of a nonaqueous phase liquid in saturated porous media." Water Resources Research **30**(2): 307-320.
- Jonker and Koelmans. (2002) Sorption of Polycyclic Aromatic Hydrocarbons and Polychlorinated Biphenyls to Soot and Soot-like Materials in the Aqueous Environment: Mechanistic Considerations. Environ. Sci. Technol. Vol. 36, No 17, 3725-3734
- Jonker, M. T. O. and A. A. Koelmans (2001). "Polyoxymethylene Solid Phase Extraction as a Partitioning Method for Hydrophobic Organic Chemicals in Sediment and Soot." Environmental Science and Technology **35**(18): 3742-3748.
- Karickhoff, S. W., D. S. Brown, et al. (1979). "Sorption of hydrophobic pollutants on natural sediments." Water Research **13**(3): 241-248.
- Khalil, M. F., U. Ghosh, et al. (2006). "Role of Weathered Coal Tar Pitch in the Partitioning of Polycyclic

- Aromatic Hydrocarbons in Manufactured Gass Plant Site Sediments." Environmental Science and Technology **40**(18): 5681-5687.
- Kim, H. S. and F. K. Pfaender (2005). "Effects of Microbially Mediated Redox Conditions on PAH-Soil Interactions." Environmental Science and Technology **39**(23): 9189-9196.
- Kim, Y. S., C. T. Jafvert, et al. (2009). "Potential consolidation-induced NAPL migration from coal tar impacted river sediment under a remediation sand cap." Journal of Hazardous Materials **162**: 1364-1370.
- Knightes, C. D. and C. A. Peters (2003). "Aqueous Phase Biodegradation Kinetics of 10 PAH Compounds." Environmental Engineering Science **20**(3): 207-218.
- Knox and Parcher. (1969) Effect of Column to Particle Diameter Ratio on Dispersion of Unsorbed Solutes in Chromatography. Analytical Chemistry. Vol. 41, No. 12. 1599-1606
- Koch, A. L. (1994). Growth Measurement. Methods in General Molecular Bacteriology. P. Gerhardt. Washington D.C., American Society of Microbiology: 248-277.
- Kreitinger, J. P., E. F. Neuhauser, et al. (2007). "Greatly Reduced Bioavailability and Toxicity of Polycyclic Aromatic Hydrocarbons to *Hyalella Azteca* in Sediments from Manufactured-Gas Plant Sites." Environmental Toxicology and Chemistry **26**(6): 1146-1157.
- Lampert, D. J. and D. Reible (2009). "An Analytical Modeling Approach for Evaluation of Capping of Contaminated Sediments." Soil and Sediment Contamination **18**: 470-488.
- Leys, N. M., L. Bastiaens, et al. (2005). "Influence of the carbon/nitrogen/phosphorous ratio on polycyclic aromatic hydrocarbon degradation by *Mycobacterium* and *Sphingomonas* in soil." Environmental Biotechnology **66**: 726-736.
- Liu, C., J. A. Jay, et al. (2001). "Capping Efficiency for Metal-Contaminated Marine Sediment under Conditions of Submarine Groundwater Discharge." Environmental Science and Technology **35**(11): 2334-2340.
- Luthy, R. G., A. Ramaswami, et al. (1993). "Interfacial Films in Coal Tar Nonaqueous-Phase Liquid-Water Systems." Environmental Science and Technology **27**(13): 2914-2918.
- Lyons, T. et al. (2006) Evaluation of Contaminant Resuspension Potential during Cap Placement at Two Dissimilar Sites. J. of Environmental Eng. April, 505-514
- Mader, B. T., K. Uwe-Goss, et al. (1997). "Sorption of Nonionic, Hydrophobic Organic Chemicals to Mineral Surfaces." Environmental Science and Technology **31**(4): 1079-1086.
- Magar, V. S. (2007). Characterization of Contaminant Transport Potential Through in-Place Sediment Caps. Society of Environmental Toxicology & Chemistry (SETAC) 28th Annual Meeting, Milwaukee, Wisconsin.
- Mayer, P., W. H. J. Vaes, et al. (2000). "Sensing Dissolved Sediment Porewater Concentrations of Persistent and Bioaccumulative Pollutants Using Disposable Solid-Phase Microextraction Fibers." Environmental Science and Technology **34**(24): 5177-5183.
- McNally, D. L., J. R. Mihelcic, et al. (1998). "Biodegradation of Three- and Four-Ring Polycyclic Aromatic Hydrocarbons under Aerobic and Denitrifying Conditions." Environmental Science and Technology **32**(17): 2633-2639.
- Mishurov, M., A. Yakirevich, et al. (2008). "Colloid Transport in a Heterogeneous Partially Saturated Sand Column." Environmental Science and Technology **42**(4): 1066-1071.
- Mohan, R. K., M. P. Brown, et al. (2000). "Design criteria and theoretical basis for capping contaminated marine sediments." Applied Ocean Research **22**: 85-93.
- Murphy, P., A. Marquette, et al. (2006). "Predicting the Performance of Activated Carbon-, Coke-, and Soil-Amended Thin Layer Sediment Caps." Journal of Environmental Engineering **132**(7): 787-794.
- Myers, M. S., B. F. Anulacion, et al. (2008). "Improved flatfish health following remediation of a PAH-contaminated site in Eagle Harbor, Washington." Aquatic Toxicology **88**: 277-288.

- Ogata, A. and R. B. Banks (1961). A Solution of the Differential Equation of Longitudinal Dispersion in Porous Media. U. S. D. o. t. Interior, United States Government Printing Office.
- Ortiz, E., M. Kraatz, et al. (1999). "Organic Phase Resistance to Dissolution of Polycyclic Aromatic Hydrocarbons." Environmental Science and Technology **33**(235-242).
- Palermo, M. R., J. E. Clausner, et al. (1998). Guidance for Subaqueous Dredged Material Capping. Dredging Operations and Environmental Research Program. Vicksburg, MS, US Army Corps of Engineers.
- Palermo, M.R., S. Maynard, J. Miller, and D. Reible. 1998. *ARCS Program: Guidance for In Situ Subaqueous Capping of Contaminated Sediments*. EPA/905/B-96/004. USEPA Great Lakes National Program Office. September.
- Paulsen, R. J., C. F. Smith, D. O'Rourke, and T. Wong. 2001. Development and Evaluation of an Ultrasonic Groundwater Seepage Meter.
- Pederson, J. A., L. E. Schweitzer, et al. (2002). "Effect of Oxidic State on Nonpolar Organic Contaminant Distribution, Mobility, and Bioavailability in Estuarine Sediments." Israel Journal of Chemistry **42**: 109-118.
- Peters, C. A., C. D. Knightes, et al. (1999). "Long-Term Compositional Dynamics of PAH-Containing NAPLs and Implications for Risk Assessment." Environmental Science and Technology **33**(24): 4499-4507.
- Piatt, J. J., D. A. Backhus, et al. (1996). "Temperature-Dependent Sorption of Naphthalene, Phenanthrene, and Pyrene to Low Organic Carbon Aquifer Sediments." Environmental Science and Technology **30**(3): 751-760.
- Pignatello, J. J. and B. Xing (1996). "Mechanisms of Slow Sorption of Organic Chemicals to Natural Particles." Environmental Science and Technology **30**(1): 1-11.
- Poerschmann, J., Z. Zhang, et al. (1997). "Solid Phase Microextraction for Determining the Distribution of Chemicals in Aqueous Matrices." Analytical Chemistry **69**: 597-600.
- Porschmann, J., F.-D. Kopinke, et al. (1998). "Solid-phase microextraction for determining the binding state of organic pollutants in contaminated water rich in humic organic matter." Journal of Chromatography A **816**: 159-167.
- Price, J. S. (2009). Solute Transport in Unsaturated Sphagnum Mosses. American Geophysical Union Joint Meeting, Toronto, ON.
- Ran, Y., B. Xing, et al. (2005). "Sorption Kinetics of Organic Contaminants by Sandy Aquifer and Its Kerogen Isolate." Environmental Science and Technology **39**(6): 1649-1657.
- Rasmussen, G., G. Fremmsvik, et al. (2002). "Treatment of creosote-contaminated groundwater in a peat/sand permeable barrier-a column study." Journal of Hazardous Materials B **93**: 285-306.
- Ripp, S., D. E. Nivens, et al. (2000). "Controlled Field Release of a Bioluminescent Genetically Engineered Microorganism for Bioremediation Process Monitoring and Control." Environmental Science and Technology **34**(5): 846-853.
- Rothermich, M. M., L. A. Hayes, et al. (2002). "Anaerobic, Sulfate-Dependent Degradation of Polycyclic Aromatic Hydrocarbons in Petroleum-Contaminated Harbor Sediment." Environmental Science and Technology **36**(22): 4811-4817.
- Sass, B. et al. Characterization of Contaminant Migration Potential Through In-Place Sediment Caps SERDP Project ID: ER-1370, Final Report - Field Studies Submitted to SERDP Apr 2009.
- Schuth, C. and P. Grathwohl (1994). Nonequilibrium transport of PAHs: A comparison of column and batch experiments. Transport and Reactive Processes in Aquifers. Rotterdam.
- Simpson, S. L., I. D. Pryor, et al. (2002). "Considerations for Capping Metal-Contaminated Sediments in Dynamic Estuarine Environments." Environmental Science and Technology **36**(17): 3772-3778.

- Stout, S. A., V. S. Magar, et al. (2001). "Characterization of Naturally-occurring and Anthropogenic PAHs in Urban Sediments--Wycoff/Eagle Harbor Superfund Site." Environmental Forensics **2**: 287-300.
- Thibodeaux, L.J.; Reible, D.; Bosworth, W.S.; Sarapas, L.C..Theoretical evaluation of the effectiveness of capping PCB contaminated New Bedford Harbor bed sediment. Report, *Louisiana State Univ. and A&M Coll., Baton Rouge (USA)* 1991, 98 pp
- Thoma, G. J., D. D. Reible, et al. (1993). "Efficiency of Capping Contaminated Sediments in Situ. 2. Mathematics of Diffusion-Adsorption in the Capping Layer " Environmental Science and Technology **27**(12): 2412-2419.
- Toride, N., F. J. Leij, et al. (1999). The CXTFIT Code for Estimating Transport Parameters from Laboratory or Field Tracer Experiments. Riverside, CA, U.S. Salinity Laboratory.
- Viana, P. Z., K. Yin, et al. (2008). "Modeling Active Capping Efficacy. 1. Metal and Organometal Contaminated Sediment Remediation." Environmental Science and Technology **42**(23): 8922-8929.
- Villholth, K. G. (1999). "Colloid Characterization and Colloid Phase Partitioning of Polycyclic Aromatic Hydrocarbons in Two Creosote-Contaminated Aquifers in Denmark." Environmental Science and Technology **33**(5): 691-699.
- Walters and Luthy. (1984) Equilibrium Adsorption of Polycyclic Aromatic Hydrocarbons from Water onto Activated Carbon. Environ. Sci. Technol. Vol. 18, No 6. 395-403
- Wammer, K. H. and C. A. Peters (2005). "Polycyclic Aromatic Hydrocarbon Biodegradation Rates: A Structure-Based Study." Environmental Science and Technology **39**(8).
- Wang, X. Q., L. J. Thibodeaux, et al. (1991). "Efficiency of Capping Contaminated Bed Sediments In Situ. 1. Laboratory-Scale Experiments on Diffusion-Adsorption in the Capping Layer." Environmental Science and Technology **25**(9): 1578-1584.
- Warith, M., L. Fernandes, et al. (1999). "Design of in-situ microbial filter for the remediation of naphthalene." Waste Management **19**: 9-25.
- White, H. K., L. XU, et al. (2005). "Abundance, Composition, and Vertical Transport of PAHs in Marsh Sediments." Environmental Science and Technology **39**(21): 8273-8280.
- Xia, X. and R. Wang (2008). "Effect of Sediment Particle Size on Polycyclic Aromatic Hydrocarbon Biodegradation: Importance of the Sediment-Water Interface." Environmental Toxicology and Chemistry **27**(1): 119-125.
- Yerushalmi, L., M. F. Manuel, et al. (1999). "Biodegradation of gasoline BTEX in a microaerophilic biobarrier." Biodegradation **10**: 341-352.
- Zhu, D. and J. J. Pignatello (2005). "Characterization of Aromatic Compound Sorptive Interactions with Black Carbon (Charcoal) Assisted by Graphite as a Model." Environmental Science and Technology **39**(7): 2033-2041.
- Zimmerman, J. R., U. Ghosh, et al. (2004). "Addition of Carbon Sorbants to Reduce PCB and PAH Bioavailability in Marine Sediments: Physicochemical Tests." Environmental Science and Technology **38**(20): 5458-5464.
- Myers, M.S. et al. (2008) Improved flatfish health following remediation of a PAH-contaminated site in Eagle Harbor, Washington. Aquatic Toxicology. Vol. 88, pp 277-288.

APPENDIX 1. Table of data used in Figures.

Figure 3. (with some additional information)

	Sediment After Mixing Before Sieving		Sediment After Sieving		Capping Material	
	ug/g	StDev	ug/g	StDev	ug/g	StDev
Naphthalene	16.2	9.1	4.8	1.3	0.002	0.0006
Acenaphthylene	14.2	1.5	6.8	1.3	0.001	0.0001
Acenaphthene	162.0	19.8	110.0	16.6	0.001	0.0003
Fluorene	76.2	9.3	53.4	7.3	0.001	0.0003
Phenanthrene	268.6	30.0	194.4	25.0	0.005	0.0013
Anthracene	64.4	11.6	114.2	7.2	0.005	0.0008
Fluoranthene	221.9	26.5	163.5	15.5	0.030	0.0071
Pyrene	152.5	18.2	128.0	27.2	0.019	0.0040
Benz(a)anthracene	30.7	3.4	22.0	2.5	0.009	0.0013
Chrysene	23.0	3.2	27.7	6.1	0.010	0.0024
Benzo(b)fluoranthene	10.1	0.9	6.9	2.5	0.005	0.0001
Benzo(k)fluoranthene	8.4	1.0	5.7	1.3	0.004	0.0000
Benzo(a)pyrene	8.3	1.0	5.5	1.1	0.004	0.0005
Indeno(1,2,3-cd)pyrene	1.7	0.3	1.1	0.1	0.002	0.0001
Dibenz(a,h)anthracene	1.3	1.2	0.5	0.0	0.000	0.0001
Benzo(g,h,i)perylene	2.9	2.4	1.2	0.1	0.001	0.0000
Totals	1062		846		0.098	

Figure 4.

Eq aqueous PAH conc, ug/L

	Sieved	Bulk
Acenaphthylene	320.14	341.61
Acenaphthene	5194.19	5373.34
Fluorene	1508.61	1435.41
Phenanthrene	2467.44	2013.79
Anthracene	343.64	290.57
Fluoranthene	484.29	359.37
Pyrene	268.49	196.38
Benz(a)anthracene	13.96	10.57
Chrysene	13.79	10.15
Benzo(b)fluoranthene	2.82	2.16
Benzo(k)fluoranthene	1.92	1.29
Benzo(a)pyrene	1.72	1.42
Indeno(1,2,3-cd)pyrene	0.00	0.51
Dibenz(a,h)anthracene	0.00	0.00
Benzo(g,h,i)perylene	0.00	0

Figure 5.

	Log(K _{TOC})	Log(K _{TOC})	Log(K _{TOC})
	Sieved	Bulk	Lit values
Acenaphthylene	4.81	4.68	-
Acenaphthene	4.63	4.68	-
Fluorene	4.93	4.97	-
Phenanthrene	5.38	5.37	5.6
Anthracene	5.62	6.02	5.8
Fluoranthene	6.07	6.03	6
Pyrene	6.17	5.68	5.9
Benz(a)anthracene	6.76	6.71	6.9
Chrysene	6.64	6.81	6.8
Benzo(b)fluoranthene	6.99	6.90	7.4
Benzo(k)fluoranthene	7.15	6.98	7.4
Benzo(a)pyrene	7.06	7.02	7.15

Figure 6a.

PAH profile through the Column 2 Dec 21, 2006 Out of linear range

calibration range

		Port	1	2	3	4	5	6
Naphthalene	5.5-1106.6		23.51	114.19	2.38			ug/L
Acenaphthylene	1.2-240.4		31.08	14.62	2.05	0.03		ug/L
Acenaphthene	1.4-293.7		641.82	268	41.16	0.07		ug/L
Fluorene	1.0-201.4		180.14	72.26	16.48	0.04	0.03	ug/L
Phenanthrene	0.73-146.8		207.61	60.28	12.46	0.26	0.24	ug/L
Anthracene	0.8-16		30.48	7.26	1.76	0.09	0.07	ug/L
Fluoranthene	0.28-56.4		59.29	4.59	1.08	0.24	0.26	ug/L
Pyrene	0.24-48		39.03	2.64	0.59	0.18	0.18	ug/L
Benzo(a)anthracene	0.01-2.2		11.92138	0.62306	0.04803			ug/L
Chrysene	0.004-0.8		5.98609	0.35727	0.03453	0.02182		ug/L

Figure 6b.

PAH profile through the Column 2 Dec 26, 2006 Out of linear range

linear range

		Port	1	2	3	5	6
Naphthalene	5.5-1106.6		11.02	42.18	76.84	86.87	86.29 ug/L
Acenaphthylene	1.2-240.4		43.47	49.44	40.96	51.31	38.59 ug/L
Acenaphthene	1.4-293.7		922.1	932.76	732.32	1034.46	765.36 ug/L
Fluorene	1.0-201.4		270.34	244.93	206.24	228.89	207.24 ug/L
Phenanthrene	0.73-146.8		282.51	244.7	212.06	196.14	219.74 ug/L
Anthracene	0.8-16		36.88	34.5	30.15	26.88	29.53 ug/L
Fluoranthene	0.28-56.4		37.48	22.16	23.12	10.64	17.03 ug/L
Pyrene	0.24-48		19.84	10.89	11.17	4.84	7.34 ug/L
Benzo(a)anthracene	0.01-2.2		0.46855	0.13196	0.07789	0.03981	0.07228 ug/L
Chrysene	0.004-0.8		0.37632	0.13112	0.10148	0.06538	0.12311 ug/L

34
26
19
15
11
7
3

8
14
17
8
25
451
812

155
135
115
97.5
87.5
77.5
67.5
58
50
42
34
26
19
15
11
7
3

996
482
522
251
279
112
55
8
26
29
11
7
8
24
24
92
726

175
155
135
115
97.5
87.5
77.5
67.5
58
50
42
34
26
19
15
11
7
3

794
43
90
58
158
14
0
3
2
1
2
0
2
4
3
2
14
115

97.5
87.5
77.5
67.5
58
50
42
34
26
19
15
11
7
3

314
191
1171
28
13
34
1
8
10
1921
1355
2499
3503
2103

87.5
77.5
67.5
58
50
42
34
26
19
15
11
7
3

627
235
1576
1062
6838
6582
243
81
43
11
6
14
610

Depth from Sediment

5
25
40
45
60

2738
4236
4483
4392
3992

57.15
49.53
41.91
34.29
19.05
11.43

1474
1806
4266
2819
6977
5492

Figure 8a.

PAH profile through Column 6 July 24, 2007 8:30 am

	calibration range	Port						6 Units
		1	2	3	4	5		
Naphthalene	5.5-2213.33	37.4	19.68	6.74	6.95	2.82	1.87 ug/L	
Acenaphthylene	1.2-481.06	44.8	33.73	5.82	2.37	0.49	0.36 ug/L	
Acenaphthene	1.4-586.67	542.1	371.63	53.54	20.99	3.5	1.55 ug/L	
Fluorene	1.0-402.67	144.19	102.86	14.25	3.77	0.76	0.36 ug/L	
Phenanthrene	0.73-293.33	154.6	108.44	18.45	2.81	0.66	0.45 ug/L	
Anthracene	0.8-32	15.97	11.94	2.27	0.43	0.13	0.13 ug/L	
Fluoranthene	0.28-112.53	22.52	13.71	2.41	0.25	0.13	0.29 ug/L	
Pyrene	0.24-96	11.27	6.65	1.15	0.16	0.1	0.23 ug/L	
Benzo(a)anthracene	0.01-4.27	0.18319	0.20591	0.04109			0.06174 ug/L	
Chrysene	0.004-1.6	0.14912	0.16345	0.05495			0.04087 ug/L	

Out of calibration range low
 Out of calibration range high

figure 8b.

PAH profile through Column 6 July 29, 2007 4:30 pm

	calibration range	Port						6 Units
		1	2	3	4	5		
Naphthalene	5.5-2213.33	9.34	18.21	20.75	21.58	40.21	25.91 ug/L	
Acenaphthylene	1.2-481.06	47.88	54.35	24.15	10.77	10.33	6.56 ug/L	
Acenaphthene	1.4-586.67	364.8	428.75	296.35	135.37	124.31	43.15 ug/L	
Fluorene	1.0-402.67	128.2	131.61	64.96	25.97	12.75	3.94 ug/L	
Phenanthrene	0.73-293.33	148.25	119.56	20.83	2.14	1.3	0.51 ug/L	
Anthracene	0.8-32	19.37	15.51	2.69	0.53	0.24	0.08 ug/L	
Fluoranthene	0.28-112.53	28.32	24.04	2.67	0.32	0.24	0.24 ug/L	
Pyrene	0.24-96	14.8	11.94	1.31	0.18	0.15	0.18 ug/L	
Benzo(a)anthracene	0.01-4.27	0.33096	0.22243				ug/L	
Chrysene	0.004-1.6	0.3072	0.2145				ug/L	

Out of calibration range low
 Out of calibration range high

Data for Initial PAH profile in 2% AC amended cap. (data in figure 9a is from a different time)

PAH profile through the Column 4 March 1, 2007

		calibration range					Units	
			Low					
			High					
	Port	1	2	3	4	5	6	
Naphthalene	5.5-2213.33	261.38	4.11	1.16		0.75	0.03	ug/L
Acenaphthylene	1.2-481.06	39.62	0.35	0.09		0.04	0	ug/L
Acenaphthene	1.4-586.67	662.31	8.29	1.71		0.58	0.02	ug/L
Fluorene	1.0-402.67	122.61	2.01	0.51		0.2	0.01	ug/L
Phenanthrene	0.73-293.33	27.14	1.41	0.67		0.36	0.04	ug/L
Anthracene	0.8-32	2.18	0.26	0.07		0.04	0	ug/L
Fluoranthene	0.28-112.53	1.22	1.37	0.14		0.06	0.01	ug/L
Pyrene	0.24-96	0.78	0.99	0.09		0.04	0.01	ug/L
Benzo(a)anthracene	0.01-4.27	0.25794	0.44811	0.02353		0.02486		ug/L
Chrysene	0.004-1.6	0.18943	0.30304	0.0317		0.02257	0.00222	ug/L

figure 9b.

PAH profile through Column 4 March 12 7:00pm, 2007

		calibration range					Units
					Out of calibration range low		
					Out of calibration range high		
	Port	1	2	3	4	6	
Naphthalene	5.5-2213.33	9.27	0.09	0.06	0.03	0.03	ug/L
Acenaphthylene	1.2-481.06	21.57	0.06	0.03	0.02	0.01	ug/L
Acenaphthene	1.4-586.67	320.03	0.23	0.1	0.04	0.03	ug/L
Fluorene	1.0-402.67	96.55	0.08	0.04	0.02	0.01	ug/L
Phenanthrene	0.73-293.33	118.93	0.3	0.14	0.06	0.03	ug/L
Anthracene	0.8-32	33	0.07	0.02	0.01	0.01	ug/L
Fluoranthene	0.28-112.53	48.54	0.27	0.07	0.03	0.02	ug/L
Pyrene	0.24-96	27.39	0.19	0.04	0.02	0.02	ug/L
Benzo(a)anthracene	0.01-4.27	0.63669	0.04873	0.00783	0.00372	0.0064	ug/L
Chrysene	0.004-1.6	0.42989	0.04411	0.0051	0.00251	0.00414	ug/L

Figure 10 (calculation of bed volumes needs to be updated slightly)

	ug/L Phen Port 1	ug/L Phen Port 6	ug/L CHR Port 1	ug/L CHR Port 6
No Amendment (Bed Volumes)				
0	207.61		5.98	
9.0742	282.51	219.74	0.3563	0.1231
38.1118	403.98	122.05	0.653	0.181
61.7049	146.78	144.28	0.884	0.198
85.2979	126.52	242.65	0.889	0.2252
137.9285	37.18	112.1	1.337	0.4044
0.2 % Peat Amendment (BV)				
0	138.61		0.288	
1.5047	154.6	0.45	0.149	0.041
3.9084	163.7	0.39	0.148	0.028
5.8627	173	0.41	0.203	
7.8169	214.34	0.64	0.375	0.065
11.9207	148.25	0.51	0.307	
13.875	237.75	0.71	0.464	
17.588	232.83	1.02	0.413	
23.0598	277.94	2.91	0.563	
58.6266	191.55	18.69	0.448	0.025
85.9857	311	71.01	0.921	0.018
91.8484	222.26	71.45	0.88	0.013
107.4821	448.64	126.74	1.48	0.015
115.299	267.62	115	1.13	0.019
136.7954	195.08	165.8	0.889	0.01

figure 11 (calculation of bed volumns needs to be corrected slightly)

	ug/L Phen Port 1	ug/L Phen Port 6	ug/L CHR Port 1	ug/L CHR Port 6
GAC 0.2% Bed Volumes				
0.1911	260.86	0.39	0.526	0.012
1.9108	237.3	0.49	0.394	
3.8216	366.8	0.51	1.875	
116.9406	4.41	0.09	0.45	7.00E-03
GAC 2% Bed Volumns				
0	27.14	0.04	0.1894	2.22E-03
5.1591	105.33	0.07		
7.8343	255.93	0.04		
13.5666	125.28	0.04	0.2854	4.98E-03
21.4009	118.93	0.03	0.4298	4.14E-03
36.3051	279.85	0.16	0.6908	0.01
40.3177	215.03	0.09	0.4825	2.57E-03
58.8524	150.12	0.02	0.303	1.50E-03
91.33	233.78	0.1	1.122	
391.7127	2.31	0.08	1.415	0.014

Figure 12

NPH ug/L	ACY ug/L	ACE ug/L	FLR ug/L	PHN ug/L	ANTH ug/L	FLN ug/L	PYR ug/L	BaA ug/L	CHR ug/L	
2.44	3.58	108.74	37.37	46.87	13.09	51.16	29.32	1.17	1.01	Sieved EH Sediment (S:L Ratio 0.04)
2.01	3.44	109.44	37.11	45.92	12.66	49.58	27.97	0.92	0.84	Sieved EH Sediment (S:L Ratio 0.04)
1.47	2.49	96.62	28.4	31.43	10.36	37.59	20.96	0.69	0.61	Sieved EH Sediment (S:L Ratio 0.04)
1.33	1.82	88.13	26.52	29.39	9.71	35.1	20.13	0.64	0.58	Sieved EH Sediment (S:L Ratio 0.04)
1.99	0.19	2.34	1.65	22.48	8.27	42.55	25.07	2.07	1.28	Column run 4 months (S:L Ratio 0.04)
1.94	0.17	2.34	1.66	22.12	7.9	39.66	23.24	1.34	0.94	Column run 4 months (S:L Ratio 0.04)
1.36	0.15	2.12	1.34	15.54	6.78	31.81	18.62	1.2	0.79	Column run 4 months (S:L Ratio 0.04)
1.19	0.06	1.86	1.16	13.61	5.71	28.58	17.08	1.38	0.88	Column run 4 months (S:L Ratio 0.04)
1.72	0.12	1.08	0.43	2.22	2.05	40.17	25.77	2.4	1.36	Column run 7 months (S:L Ratio 0.04)
1.68	0.11	0.97	0.39	2.04	1.69	35.39	22.79	1.61	1.05	Column run 7 months (S:L Ratio 0.04)
1.17	0.09	0.93	0.32	1.45	1.5	29.18	18.56	1.44	0.85	Column run 7 months (S:L Ratio 0.04)
1.16	0.11	0.93	0.32	1.47	1.51	29.51	19.04	1.66	1	Column run 7 months (S:L Ratio 0.04)

Figure 13

	<u>Initial</u>	<u>ug/L</u>	<u>18 days</u>	<u>ug/L</u>
BOD Solution	average	0.733333	average	0.04
	stdev	0.051316	stdev	0.014142
BOD Solution (4xspike)	average	2.936667	average	0.045
	stdev	0.090738	stdev	0.007071
BOD with NaN3	average	0.983333	average	0.25
	stdev	0.032146	stdev	0.042426
My Nutrient Mix	average	1.246667	average	0.045
	stdev	0.046188	stdev	0.007071

Figure 14

Days	ug/L		ug/L	
	Living	stdev	Killed	stdev
0	286.57	18.89	472.11	18.52
4	98.46	0.73	134.28	10.06
10	0.11	0.02	81.35	6.00

Figure 15

	Port 1	Port 2	Port 3	Port 4	Port 5	
	Distance from Sediment					
BV	1cm	16cm	31cm	46cm	61cm	Overlying Water
0	15.96	0.59	0.17	0.19	0.03	
0.9	42.29	9.84	3.29	0	0	
1.9	53.43	29.82	26.46	14.24	0.67	
8.1	10.42	7.58	4.66	0.54	0.06	3.95
15.5	1.91	10.39	26.17	24.59	16.15	4.56
21	1.01	1.34	14.41	15.15	11.26	0.58
24.7	0.77	0.8	13.71	12.63	6.43	10.87
37.9	0.77	0.13	0.79	0.73	0.49	1
63.1	0.39	0.09	0.07	0.05	0.06	0.46
90.7	0	2.51	0	0	0.05	

Figure 18

No Amendment		Peat Amendment	
Minutes	Concentration (C/Co)	Minutes	Concentration (C/Co)
0	0.0115	450.6	0.0253
30	0.0166	510.6	0.0383
90	0.021	573	0.092
156.9	0.0207	635.4	0.202
222.9	0.02	702.9	0.389
284.4	0.019	768	0.58
343.8	0.0142	818.1	0.716
382.8	0.0153	869.1	0.8
403.8	0.018	935.7	0.8766
445.8	0.0217	1008.3	0.9367
510.3	0.0356	1076.4	0.9667
571.8	0.0827	1134.9	0.9967
642.9	0.1875	1195.2	1
716.4	0.3641		
778.8	0.518		
832.8	0.6231		
883.8	0.7247		
940.8	0.8163		
988.8	0.8468		
1027.8	0.8671		
1075.8	0.9214		
1123.8	0.9112		
1156.8	0.9101		

**Figure 20, 1st Biological Column Data and Model
CXTFIT**

degradation rate for these simulations = 0.0447 day⁻¹ (Based on Peters et al. 1999, ES&T, 33, 4499)

model Bed Volume degradation	model [ug/L] degradation	data Bed Volume	data [ug/L]	model Bed Volume no degradation	model [ug/L] no degradation
0	0.26	0	0	0.16	0
1.89	0.3761	0.87	0.87	0.13	1.89
3.78	2.5313	1.89	1.89	0.74	3.78
5.67	6.3412	8.1	8.1	0.13	5.67
7.56	12.013	15.5	15.5	16.22	7.56
9.45	21.085	21	21	11.35	9.45
11.34	34.651	24.7	24.7	6.49	11.34
13.23	52.989	37.9	37.9	1.52	13.23
15.12	74.039				15.12
17.01	93.599				17.01
18.9	107.52				18.9
20.79	113.62				20.79
22.68	112.08				22.68
24.57	104.72				24.57
26.46	93.914				26.46
28.35	81.718				28.35
30.24	69.506				30.24
32.13	58.013				32.13
34.02	47.582				34.02
35.91	38.36				35.91
37.8	30.396				37.8

Figure 21 (phenanthrene, constant input)
CXTFIT

Darcy velocity = 0.015 m/hr

Bed Volumes [ug/L]		Bed Volumes [ug/L]	
No Degradation	No Degradation	Degradation	Degradation
0	0	0	0
0.5556	0	0.5556	0
1.1111	1.77E-17	1.1111	1.76E-17
1.6667	1.12E-09	1.6667	1.12E-09
2.2222	7.51E-06	2.2222	7.46E-06
2.7778	1.27E-03	2.7778	1.26E-03
3.3333	0.0337	3.3333	0.0334
3.8889	0.3124	3.8889	0.3091
4.4444	1.4963	4.4444	1.4787
5	4.6302	5	4.5699
5.5556	10.584	5.5556	10.433
6.1111	19.483	6.1111	19.183
6.6667	30.607	6.6667	30.103
7.2222	42.743	7.2222	41.998
7.7778	54.653	7.7778	53.653
8.3333	65.401	8.3333	64.154
8.8889	74.467	8.8889	72.998
9.4444	81.705	9.4444	80.048
10	87.228	10	85.417
10.5556	91.284	10.5556	89.355
11.1111	94.17	11.1111	92.153
11.6667	96.169	11.6667	94.087
12.2222	97.521	12.2222	95.393
12.7778	98.418	12.7778	96.258
13.3333	99.003	13.3333	96.821
13.8889	99.378	13.8889	97.182
14.4444	99.616	14.4444	97.411
15	99.765	15	97.553
15.5556	99.857	15.5556	97.642
16.1111	99.914	16.1111	97.696
16.6667	99.948	16.6667	97.729
17.2222	99.969	17.2222	97.748
17.7778	99.982	17.7778	97.76
18.3333	99.989	18.3333	97.767
18.8889	99.994	18.8889	97.772
19.4444	99.996	19.4444	97.774
20	99.998	20	97.776

Darcy velocity = 0.00015 m/hr

Bed Volumes [ug/L]		Bed Volumes [ug/L]	
No Degradation	No Degradation	Degradation	Degradation
0	0	0	0
0.5539	1.5215	0.5539	1.3569
1.1077	5.1481	1.1077	4.2061
1.6616	8.7974	1.6616	6.6542
2.2155	12.169	2.2155	8.5812
2.7693	15.25	2.7693	10.082
3.3232	18.074	3.3232	11.253
3.877	20.677	3.877	12.172
4.4309	23.087	4.4309	12.897
4.9848	25.332	4.9848	13.472
5.5386	27.432	5.5386	13.93
6.0925	29.403	6.0925	14.297
6.6464	31.261	6.6464	14.591
7.2002	33.018	7.2002	14.828
7.7541	34.683	7.7541	15.019
8.3079	36.265	8.3079	15.174
8.8618	37.772	8.8618	15.299
9.4157	39.21	9.4157	15.401
9.9695	40.584	9.9695	15.484
10.5234	41.9	10.5234	15.552
11.0773	43.163	11.0773	15.607
11.6311	44.375	11.6311	15.653
12.185	45.54	12.185	15.69
12.7389	46.662	12.7389	15.72
13.2927	47.743	13.2927	15.745
13.8466	48.786	13.8466	15.765
14.4004	49.793	14.4004	15.782
14.9543	50.767	14.9543	15.796
15.5082	51.708	15.5082	15.808
16.062	52.619	16.062	15.817
16.6159	53.502	16.6159	15.825
17.1698	54.357	17.1698	15.831
17.7236	55.187	17.7236	15.837
18.2775	55.992	18.2775	15.841
18.8313	56.774	18.8313	15.845
19.3852	57.534	19.3852	15.848
19.9391	58.273	19.9391	15.85
20.4929	58.991	20.4929	15.852

Figure 22
CXTFIT

note: unlike figure 6M, these simulations assume linear partitioning for AC, log Kd = 8.76 (Jonker and Koelmans, 2002, ES&T 36, 3725-3734)

Bed Volumes	[ug/L]								
0.0538	0	0.0538	0	0.0538	0	0.0571	0	0.0571	0
0.5376	0	2.6882	0	2.6882	0	57142.8571	0	57.1429	0
1.0753	0	5.3763	0	5.3763	0	114285.7143	0	114.2857	0
1.6129	0	8.0645	0	8.0645	0	171428.5714	0	171.4286	0
2.1505	0	10.7527	0	10.7527	0	228571.4286	0	228.5714	0
2.6882	0	13.4409	0	13.4409	0	285714.2857	0	285.7143	0
3.2258	0	16.129	6.45E-12	16.129	0	342857.1429	0	342.8571	0
3.7634	0	18.8172	5.58E-09	18.8172	0	400000	0	400	0
4.3011	0	21.5054	7.90E-07	21.5054	0	457142.8571	0	457.1429	0
4.8387	0	24.1935	3.34E-05	24.1935	0	514285.7143	3.22E-13	514.2857	2.66E-13
5.3763	0	26.8817	6.09E-04	26.8817	0	571428.5714	5.20E-11	571.4286	4.36E-11
5.914	0	29.5699	6.01E-03	29.5699	0	628571.4286	3.16E-09	628.5714	2.69E-09
6.4516	5.55E-15	32.2581	0.0375	32.2581	0	685714.2857	9.20E-08	685.7143	7.97E-08
6.9892	5.33E-13	34.9462	0.1642	34.9462	0	742857.1429	1.52E-06	742.8571	1.34E-06
7.5269	1.94E-11	37.6344	0.5467	37.6344	0	800000	1.62E-05	800	1.44E-05
8.0645	4.27E-10	40.3226	1.462	40.3226	0	857142.8571	1.21E-04	857.1429	1.08E-04
8.6022	6.22E-09	43.0108	3.2769	43.0108	0	914285.7143	6.74E-04	914.2857	6.10E-04
9.1398	6.45E-08	45.6989	6.3606	45.6989	0	971428.5714	2.97E-03	971.4286	2.71E-03
9.6774	5.04E-07	48.3871	10.9689	48.3871	0	1028571.429	0.0107	1028.5714	9.88E-03
10.2151	3.10E-06	51.0753	17.1521	51.0753	0	1085714.286	0.0329	1085.7143	0.0305
10.7527	1.56E-05	53.7634	24.725	53.7634	2.22E-14	1142857.143	0.0877	1142.8571	0.0816
11.2903	6.59E-05	56.4516	33.3046	56.4516	3.22E-13	1200000	0.2069	1200	0.1937
11.828	2.40E-04	59.1398	42.3943	59.1398	3.25E-12	1257142.857	0.4403	1257.1429	0.4143
12.3656	7.65E-04	61.828	51.4809	61.828	2.67E-11	1314285.714	0.8565	1314.2857	0.8097
12.9032	2.18E-03	64.5161	60.1158	64.5161	1.82E-10	1371428.571	1.5408	1371.4286	1.4631
13.4409	5.62E-03	67.2043	67.9649	67.2043	1.06E-09	1428571.429	2.5883	1428.5714	2.4679
13.9785	0.0133	69.8925	74.8259	69.8925	5.29E-09	1485714.286	4.0941	1485.7143	3.9186
14.5161	0.0289	72.5806	80.6187	72.5806	2.33E-08	1542857.143	6.141	1542.8571	5.8988
15.0538	0.0588	75.2688	85.3609	75.2688	9.15E-08	1600000	8.7884	1600	8.4701
15.5914	0.1123	77.957	89.1376	77.957	3.24E-07	1657142.857	12.0635	1657.1429	11.663
16.129	0.2027	80.6452	92.0717	80.6452	1.05E-06	1714285.714	15.9564	1714.2857	15.4719
16.6667	0.3477	83.3333	94.301	83.3333	3.10E-06	1771428.571	20.4198	1771.4286	19.8542
17.2043	0.5698	86.0215	95.9611	86.0215	8.53E-06	1828571.429	25.3736	1828.5714	24.7342
17.7419	0.8956	88.7097	97.1749	88.7097	2.19E-05	1885714.286	30.7115	1885.7143	30.0096
18.2796	1.3555	91.3978	98.0478	91.3978	5.28E-05	1942857.143	36.3108	1942.8571	35.5605
18.8172	1.9821	94.086	98.6661	94.086	1.20E-04	2000000	42.0421	2000	41.2594
19.3548	2.8086	96.7742	99.0981	96.7742	2.59E-04	2057142.857	47.7782	2057.1429	46.9798
19.8925	3.8667	99.4624	99.3961	99.4624	5.33E-04	2114285.714	53.4024	2114.2857	52.6046
20.4301	5.1851	102.1505	99.5992	102.1505	1.05E-03	2171428.571	58.8136	2171.4286	58.0312
20.9677	6.7867	104.8387	99.7363	104.8387	1.98E-03	2228571.429	63.9298	2228.5714	63.1759
21.5054	8.6879	107.5269	99.8278	107.5269	3.60E-03	2285714.286	68.6901	2285.7143	67.9753
22.043	10.8965	110.2151	99.8884	110.2151	6.31E-03	2342857.143	73.0537	2342.8571	72.386
22.5806	13.4115	112.9032	99.9282	112.9032	0.0107	2400000	76.999	2400	76.3839
23.1183	16.2229	115.5914	99.9541	115.5914	0.0176	2457142.857	80.5206	2457.1429	79.9613
23.6559	19.3119	118.2796	99.9708	118.2796	0.0282	2514285.714	83.6268	2514.2857	83.1244
24.1935	22.6517	120.9677	99.9815	120.9677	0.044	2571428.571	86.3364	2571.4286	85.8901
24.7312	26.209	123.6559	99.9884	123.6559	0.0669	2628571.429	88.6757	2628.5714	88.2833
25.2688	29.9452	126.3441	99.9927	126.3441	0.0995	2685714.286	90.6759	2685.7143	90.3343
25.8065	33.8181	129.0323	99.9955	129.0323	0.1448	2742857.143	92.3706	2742.8571	92.076
26.3441	37.7834	131.7204	99.9972	131.7204	0.2064	2800000	93.7944	2800	93.5425
26.8817	41.7968	134.4086	99.9983	134.4086	0.2887	2857142.857	94.981	2857.1429	94.7675
27.4194	45.815	137.0968	99.9989	137.0968	0.3966	2914285.714	95.9627	2914.2857	95.783
27.957	49.7971	139.7849	99.9993	139.7849	0.5359	2971428.571	96.7691	2971.4286	96.6189
28.4946	53.7055	142.4731	99.9996	142.4731	0.7126	3028571.429	97.4271	3028.5714	97.3025
29.0323	57.5068	145.1613	99.9998	145.1613	0.9337	3085714.286	97.9607	3085.7143	97.858
29.5699	61.1726	147.8495	99.9999	147.8495	1.2062	3142857.143	98.3909	3142.8571	98.3067
30.1075	64.6789	150.5376	99.9999	150.5376	1.5377	3200000	98.7357	3200	98.6671
30.6452	68.0071	153.2258	99.9999	153.2258	1.9359	3257142.857	99.0107	3257.1429	98.9551
31.1828	71.1434	155.914	100	155.914	2.4083	3314285.714	99.2289	3314.2857	99.1841
31.7204	74.0786	158.6022	100	158.6022	2.9625	3371428.571	99.4012	3371.4286	99.3652
32.2581	76.8075	161.2903	100	161.2903	3.6057	3428571.429	99.5366	3428.5714	99.5079
32.7957	79.3291	163.9785	100	163.9785	4.3445	3485714.286	99.6427	3485.7143	99.6198
33.3333	81.6452	166.6667	100	166.6667	5.1847	3542857.143	99.7253	3542.8571	99.7073
33.871	83.7609	169.3548	100	169.3548	6.1315	3600000	99.7895	3600	99.7753
34.4086	85.683	172.043	100	172.043	7.189	3657142.857	99.8392	3657.1429	99.828
34.9462	87.4204	174.7312	100	174.7312	8.3601	3714285.714	99.8775	3714.2857	99.8687
35.4839	88.9833	177.4194	100	177.4194	9.6465	3771428.571	99.9069	3771.4286	99.9001
36.0215	90.3827	180.1075	100	180.1075	11.0489	3828571.429	99.9295	3828.5714	99.9242
36.5591	91.6302	182.7957	100	182.7957	12.5665	3885714.286	99.9467	3885.7143	99.9426
37.0968	92.7375	185.4839	100	185.4839	14.1971	3942857.143	99.9598	3942.8571	99.9566
37.6344	93.7164	188.172	100	188.172	15.9375	4000000	99.9698	4000	99.9673
38.172	94.5785	190.8602	100	190.8602	17.7832	4057142.857	99.9773	4057.1429	99.9754
38.7097	95.3349	193.5484	100	193.5484	19.7284	4114285.714	99.983	4114.2857	99.9816
39.2473	95.9962	196.2366	100	196.2366	21.7666	4171428.571	99.9873	4171.4286	99.9862
39.7849	96.5724	198.9247	100	198.9247	23.89	4228571.429	99.9905	4228.5714	99.9897
40.3226	97.0728	201.6129	100	201.6129	26.0902	4285714.286	99.9929	4285.7143	99.9923
40.8602	97.5061	204.3011	100	204.3011	28.3582	4342857.143	99.9948	4342.8571	99.9943
41.3978	97.88	206.9892	100	206.9892	30.6843	4400000	99.9961	4400	99.9957
41.9355	98.2019	209.6774	100	209.6774	33.0587	4457142.857	99.9971	4457.1429	99.9968
42.4731	98.4781	212.3656	100	212.3656	35.471	4514285.714	99.9979	4514.2857	99.9977
43.0108	98.7146	215.0538	100	215.0538	37.9111	4571428.571	99.9984	4571.4286	99.9983
43.5484	98.9165	217.7419	100	217.7419	40.3687	4628571.429	99.9988	4628.5714	99.9987
44.086	99.0884	220.4301	100	220.4301	42.8337	4685714.286	99.9991	4685.7143	99.9991

44.6237	99.2345	223.1183	100	223.1183	45.2965	4742857.143	99.9994	4742.8571	99.9993
45.1613	99.3584	225.8065	100	225.8065	47.7474	4800000	99.9995	4800	99.9995
45.6989	99.4631	228.4946	100	228.4946	50.1778	4857142.857	99.9997	4857.1429	99.9996
46.2366	99.5515	231.1828	100	231.1828	52.5791	4914285.714	99.9998	4914.2857	99.9997
46.7742	99.626	233.871	100	233.871	54.9436	4971428.571	99.9998	4971.4286	99.9998
47.3118	99.6886	236.5591	100	236.5591	57.2641	5028571.429	99.9999	5028.5714	99.9999
47.8495	99.7412	239.2473	100	239.2473	59.5342	5085714.286	99.9999	5085.7143	99.9999
48.3871	99.7851	241.9355	100	241.9355	61.7482	5142857.143	99.9999	5142.8571	99.9999
48.9247	99.8219	244.6237	100	244.6237	63.9009	5200000	99.9999	5200	99.9999
49.4624	99.8526	247.3118	100	247.3118	65.988	5257142.857	100	5257.1429	100
50	99.8782	250	100	250	68.006	5314285.714	100	5314.2857	100
50.5376	99.8994	252.6882	100	252.6882	69.9517	5371428.571	100	5371.4286	100
51.0753	99.9171	255.3763	100	255.3763	71.8229	5428571.429	100	5428.5714	100
51.6129	99.9317	258.0645	100	258.0645	73.6179	5485714.286	100	5485.7143	100
52.1505	99.9439	260.7527	100	260.7527	75.3356	5542857.143	100	5542.8571	100
52.6882	99.9539	263.4409	100	263.4409	76.9754	5600000	100	5600	100
53.2258	99.9622	266.129	100	266.129	78.5373	5657142.857	100	5657.1429	100
53.7634	99.969	268.8172	100	268.8172	80.0216	5714285.714	100	5714.2857	100
54.3011	99.9746	271.5054	100	271.5054	81.4291	5771428.571	100	5771.4286	100
54.8387	99.9793	274.1935	100	274.1935	82.761	5828571.429	100	5828.5714	100
55.3763	99.9831	276.8817	100	276.8817	84.0188	5885714.286	100	5885.7143	100
55.914	99.9862	279.5699	100	279.5699	85.2043	5942857.143	100	5942.8571	100
56.4516	99.9887	282.2581	100	282.2581	86.3194	6000000	100	6000	100
56.9892	99.9908	284.9462	100	284.9462	87.3665	6057142.857	100	6057.1429	100
57.5269	99.9925	287.6344	100	287.6344	88.3478	6114285.714	100	6114.2857	100
58.0645	99.9939	290.3226	100	290.3226	89.266	6171428.571	100	6171.4286	100
58.6022	99.9951	293.0108	100	293.0108	90.1235	6228571.429	100	6228.5714	100
59.1398	99.996	295.6989	100	295.6989	90.9231	6285714.286	100	6285.7143	100
59.6774	99.9968	298.3871	100	298.3871	91.6675	6342857.143	100	6342.8571	100
60.2151	99.9974	301.0753	100	301.0753	92.3594	6400000	100	6400	100
60.7527	99.9979	303.7634	100	303.7634	93.0015	6457142.857	100	6457.1429	100
61.2903	99.9983	306.4516	100	306.4516	93.5965	6514285.714	100	6514.2857	100
61.828	99.9986	309.1398	100	309.1398	94.147	6571428.571	100	6571.4286	100
62.3656	99.9989	311.828	100	311.828	94.6558	6628571.429	100	6628.5714	100
62.9032	99.9991	314.5161	100	314.5161	95.1252	6685714.286	100	6685.7143	100
63.4409	99.9993	317.2043	100	317.2043	95.5578	6742857.143	100	6742.8571	100
63.9785	99.9994	319.8925	100	319.8925	95.9559	6800000	100	6800	100
64.5161	99.9995	322.5806	100	322.5806	96.3218	6857142.857	100	6857.1429	100
65.0538	99.9996	325.2688	100	325.2688	96.6578	6914285.714	100	6914.2857	100
65.5914	99.9997	327.957	100	327.957	96.9658	6971428.571	100	6971.4286	100
66.129	99.9998	330.6452	100	330.6452	97.2478	7028571.429	100	7028.5714	100
66.6667	99.9998	333.3333	100	333.3333	97.5059	7085714.286	100	7085.7143	100
67.2043	99.9998	336.0215	100	336.0215	97.7417	7142857.143	100	7142.8571	100
67.7419	99.9999	338.7097	100	338.7097	97.9569	7200000	100	7200	100
68.2796	99.9999	341.3978	100	341.3978	98.1531	7257142.857	100	7257.1429	100
68.8172	99.9999	344.086	100	344.086	98.3318	7314285.714	100	7314.2857	100
69.3548	99.9999	346.7742	100	346.7742	98.4944	7371428.571	100	7371.4286	100
69.8925	99.9999	349.4624	100	349.4624	98.6422	7428571.429	100	7428.5714	100
70.4301	100	352.1505	100	352.1505	98.7764	7485714.286	100	7485.7143	100
70.9677	100	354.8387	100	354.8387	98.8982	7542857.143	100	7542.8571	100
71.5054	100	357.5269	100	357.5269	99.0086	7600000	100	7600	100
72.043	100	360.2151	100	360.2151	99.1086	7657142.857	100	7657.1429	100
72.5806	100	362.9032	100	362.9032	99.199	7714285.714	100	7714.2857	100
73.1183	100	365.5914	100	365.5914	99.2808	7771428.571	100	7771.4286	100
73.6559	100	368.2796	100	368.2796	99.3546	7828571.429	100	7828.5714	100
74.1935	100	370.9677	100	370.9677	99.4213	7885714.286	100	7885.7143	100
74.7312	100	373.6559	100	373.6559	99.4814	7942857.143	100	7942.8571	100
75.2688	100	376.3441	100	376.3441	99.5355	8000000	100	8000	100
75.8065	100	379.0323	100	379.0323	99.5843	8057142.857	100	8057.1429	100
76.3441	100	381.7204	100	381.7204	99.6282	8114285.714	100	8114.2857	100
76.8817	100	384.4086	100	384.4086	99.6676	8171428.571	100	8171.4286	100
77.4194	100	387.0968	100	387.0968	99.703	8228571.429	100	8228.5714	100
77.957	100	389.7849	100	389.7849	99.7349	8285714.286	100	8285.7143	100
78.4946	100	392.4731	100	392.4731	99.7634	8342857.143	100	8342.8571	100
79.0323	100	395.1613	100	395.1613	99.789	8400000	100	8400	100
79.5699	100	397.8495	100	397.8495	99.8119	8457142.857	100	8457.1429	100
80.1075	100	400.5376	100	400.5376	99.8324	8514285.714	100	8514.2857	100
80.6452	100	403.2258	100	403.2258	99.8508	8571428.571	100	8571.4286	100
81.1828	100	405.914	100	405.914	99.8672	8628571.429	100	8628.5714	100
81.7204	100	408.6022	100	408.6022	99.8819	8685714.286	100	8685.7143	100
82.2581	100	411.2903	100	411.2903	99.895	8742857.143	100	8742.8571	100
82.7957	100	413.9785	100	413.9785	99.9067	8800000	100	8800	100
83.3333	100	416.6667	100	416.6667	99.9171	8857142.857	100	8857.1429	100
83.871	100	419.3548	100	419.3548	99.9264	8914285.714	100	8914.2857	100
84.4086	100	422.043	100	422.043	99.9347	8971428.571	100	8971.4286	100
84.9462	100	424.7312	100	424.7312	99.9421	9028571.429	100	9028.5714	100
85.4839	100	427.4194	100	427.4194	99.9486	9085714.286	100	9085.7143	100
86.0215	100	430.1075	100	430.1075	99.9545	9142857.143	100	9142.8571	100
86.5591	100	432.7957	100	432.7957	99.9597	9200000	100	9200	100
87.0968	100	435.4839	100	435.4839	99.9643	9257142.857	100	9257.1429	100
87.6344	100	438.172	100	438.172	99.9684	9314285.714	100	9314.2857	100
88.172	100	440.8602	100	440.8602	99.972	9371428.571	100	9371.4286	100
88.7097	100	443.5484	100	443.5484	99.9753	9428571.429	100	9428.5714	100
89.2473	100	446.2366	100	446.2366	99.9781	9485714.286	100	9485.7143	100
89.7849	100	448.9247	100	448.9247	99.9807	9542857.143	100	9542.8571	100
90.3226	100	451.6129	100	451.6129	99.9829	9600000	100	9600	100
90.8602	100	454.3011	100	454.3011	99.9849	9657142.857	100	9657.1429	100

91.3978	100	456.9892	100	456.9892	99.9867	9714285.714	100	9714.2857	100
91.9355	100	459.6774	100	459.6774	99.9883	9771428.571	100	9771.4286	100
92.4731	100	462.3656	100	462.3656	99.9897	9828571.429	100	9828.5714	100
93.0108	100	465.0538	100	465.0538	99.9909	9885714.286	100	9885.7143	100
93.5484	100	467.7419	100	467.7419	99.992	9942857.143	100	9942.8571	100
94.086	100	470.4301	100	470.4301	99.9929	10000000	100	10000	100
94.6237	100	473.1183	100	473.1183	99.9938	10057142.86	100	10057.1429	100
95.1613	100	475.8065	100	475.8065	99.9945	10114285.71	100	10114.2857	100
95.6989	100	478.4946	100	478.4946	99.9952	10171428.57	100	10171.4286	100
96.2366	100	481.1828	100	481.1828	99.9957	10228571.43	100	10228.5714	100
96.7742	100	483.871	100	483.871	99.9963	10285714.29	100	10285.7143	100
97.3118	100	486.5591	100	486.5591	99.9967	10342857.14	100	10342.8571	100
97.8495	100	489.2473	100	489.2473	99.9971	10400000	100	10400	100
98.3871	100	491.9355	100	491.9355	99.9975	10457142.86	100	10457.1429	100
98.9247	100	494.6237	100	494.6237	99.9978	10514285.71	100	10514.2857	100
99.4624	100	497.3118	100	497.3118	99.998	10571428.57	100	10571.4286	100
100	100	500	100	500	99.9983	10628571.43	100	10628.5714	100
100.5376	100	502.6882	100	502.6882	99.9985	10685714.29	100	10685.7143	100
101.0753	100	505.3763	100	505.3763	99.9987	10742857.14	100	10742.8571	100
101.6129	100	508.0645	100	508.0645	99.9988	10800000	100	10800	100
102.1505	100	510.7527	100	510.7527	99.999	10857142.86	100	10857.1429	100
102.6882	100	513.4409	100	513.4409	99.9991	10914285.71	100	10914.2857	100
103.2258	100	516.129	100	516.129	99.9992	10971428.57	100	10971.4286	100
103.7634	100	518.8172	100	518.8172	99.9993	11028571.43	100	11028.5714	100
104.3011	100	521.5054	100	521.5054	99.9994	11085714.29	100	11085.7143	100
104.8387	100	524.1935	100	524.1935	99.9995	11142857.14	100	11142.8571	100
105.3763	100	526.8817	100	526.8817	99.9995	11200000	100	11200	100
105.914	100	529.5699	100	529.5699	99.9996	11257142.86	100	11257.1429	100
106.4516	100	532.2581	100	532.2581	99.9996	11314285.71	100	11314.2857	100
106.9892	100	534.9462	100	534.9462	99.9997	11371428.57	100	11371.4286	100
107.5269	100	537.6344	100	537.6344	99.9997	11428571.43	100	11428.5714	100
108.0645	100	540.3226	100	540.3226	99.9998	11485714.29	100	11485.7143	100
108.6022	100	543.0108	100	543.0108	99.9998	11542857.14	100	11542.8571	100
109.1398	100	545.6989	100	545.6989	99.9998	11600000	100	11600	100
109.6774	100	548.3871	100	548.3871	99.9998	11657142.86	100	11657.1429	100
110.2151	100	551.0753	100	551.0753	99.9999	11714285.71	100	11714.2857	100
110.7527	100	553.7634	100	553.7634	99.9999	11771428.57	100	11771.4286	100
111.2903	100	556.4516	100	556.4516	99.9999	11828571.43	100	11828.5714	100
111.828	100	559.1398	100	559.1398	99.9999	11885714.29	100	11885.7143	100
112.3656	100	561.828	100	561.828	99.9999	11942857.14	100	11942.8571	100
112.9032	100	564.5161	100	564.5161	99.9999	12000000	100	12000	100
113.4409	100	567.2043	100	567.2043	99.9999	12057142.86	100	12057.1429	100
113.9785	100	569.8925	100	569.8925	99.9999	12114285.71	100	12114.2857	100
114.5161	100	572.5806	100	572.5806	100	12171428.57	100	12171.4286	100
115.0538	100	575.2688	100	575.2688	100	12228571.43	100	12228.5714	100
115.5914	100	577.957	100	577.957	100	12285714.29	100	12285.7143	100
116.129	100	580.6452	100	580.6452	100	12342857.14	100	12342.8571	100
116.6667	100	583.3333	100	583.3333	100	12400000	100	12400	100
117.2043	100	586.0215	100	586.0215	100	12457142.86	100	12457.1429	100
117.7419	100	588.7097	100	588.7097	100	12514285.71	100	12514.2857	100
118.2796	100	591.3978	100	591.3978	100	12571428.57	100	12571.4286	100
118.8172	100	594.086	100	594.086	100	12628571.43	100	12628.5714	100
119.3548	100	596.7742	100	596.7742	100	12685714.29	100	12685.7143	100
119.8925	100	599.4624	100	599.4624	100	12742857.14	100	12742.8571	100
120.4301	100	602.1505	100	602.1505	100	12800000	100	12800	100
120.9677	100	604.8387	100	604.8387	100	12857142.86	100	12857.1429	100
121.5054	100	607.5269	100	607.5269	100	12914285.71	100	12914.2857	100
122.043	100	610.2151	100	610.2151	100	12971428.57	100	12971.4286	100
122.5806	100	612.9032	100	612.9032	100	13028571.43	100	13028.5714	100
123.1183	100	615.5914	100	615.5914	100	13085714.29	100	13085.7143	100
123.6559	100	618.2796	100	618.2796	100	13142857.14	100	13142.8571	100
124.1935	100	620.9677	100	620.9677	100	13200000	100	13200	100
124.7312	100	623.6559	100	623.6559	100	13257142.86	100	13257.1429	100
125.2688	100	626.3441	100	626.3441	100	13314285.71	100	13314.2857	100
125.8065	100	629.0323	100	629.0323	100	13371428.57	100	13371.4286	100
126.3441	100	631.7204	100	631.7204	100	13428571.43	100	13428.5714	100
126.8817	100	634.4086	100	634.4086	100	13485714.29	100	13485.7143	100
127.4194	100	637.0968	100	637.0968	100	13542857.14	100	13542.8571	100
127.957	100	639.7849	100	639.7849	100	13600000	100	13600	100
128.4946	100	642.4731	100	642.4731	100	13657142.86	100	13657.1429	100
129.0323	100	645.1613	100	645.1613	100	13714285.71	100	13714.2857	100
129.5699	100	647.8495	100	647.8495	100	13771428.57	100	13771.4286	100
130.1075	100	650.5376	100	650.5376	100	13828571.43	100	13828.5714	100
130.6452	100	653.2258	100	653.2258	100	13885714.29	100	13885.7143	100
131.1828	100	655.914	100	655.914	100	13942857.14	100	13942.8571	100
131.7204	100	658.6022	100	658.6022	100	14000000	100	14000	100
132.2581	100	661.2903	100	661.2903	100	14057142.86	100	14057.1429	100
132.7957	100	663.9785	100	663.9785	100	14114285.71	100	14114.2857	100
133.3333	100	666.6667	100	666.6667	100	14171428.57	100	14171.4286	100
133.871	100	669.3548	100	669.3548	100	14228571.43	100	14228.5714	100
134.4086	100	672.043	100	672.043	100	14285714.29	100	14285.7143	100
134.9462	100	674.7312	100	674.7312	100	14342857.14	100	14342.8571	100
135.4839	100	677.4194	100	677.4194	100	14400000	100	14400	100
136.0215	100	680.1075	100	680.1075	100	14457142.86	100	14457.1429	100
136.5591	100	682.7957	100	682.7957	100	14514285.71	100	14514.2857	100
137.0968	100	685.4839	100	685.4839	100	14571428.57	100	14571.4286	100
47430000	100	47430000	100	47430000	100	44625000	100	44625000	100

MODEL PARAMETERS

	Cap with: No Amendment		Cap with: 0.2% TOC Amendment		Cap with: 2% GAC Amendment	
		std error ⁺		std error ⁺		
Bulk Density, kg/L	1.6		1.13		1.65	
Effective Porosity	0.28	0.001	0.26	0.0007	0.28	
longitudinal dispersivity, cm	1.65	0.09	1.08	0.04	1.65	
flux, Darcy velocity, cm/day	31		32		32	
Kd Phenanthrene, L/kg	4.73		22.23			
Kd Pyrene, L/kg	24		162.4			
Kfr Phenanthrene, (mg/Kg)/(mg/L) ^{1/n}					53703.2	
n, Phenanthrene					0.41	